Synthesis, and biological evaluation of EGFR/HER2-NAMPT conjugates for tumor treatment

Mengyuan Ding

East China Normal University

Qianqian Shen

Chinese Academy of Sciences

Wei Lu

East China Normal University

Shulei Zhu (✉ slzhu@chem.ecnu.edu.cn)

East China Normal University

Research Article

Additional Declarations: No competing interests reported.

Abstract

Throughout the reported applications of EGFR inhibitors, it is usually employed with HDAC or other targets to design multi-target inhibitors for cancer treatment. In this paper, we designed a drug conjugate that targeted EGFR&HER2 and had inhibitory activity of NAMPT simultaneously. Compound **20c** significantly inhibited the EGFR&HER2 and NAMPT enzyme activities, and had comparable or even higher anti-proliferative activity than lapatinib in various cancer cells with over-expressed EGFR and HER2. Importantly, **20c** was expected to overcome resistance to traditional EGFR inhibitors, so as to obtain better curative effect. This strategy is a promising method of embedding multiple pharmacophores into a single molecule, which lays a good foundation for the design and synthesis of small molecule drug conjugates with strong targeting ability and high cytotoxicity.

1. Introduction

The tumor-selective drug delivery system consists of targeting moieties, such as monoclonal antibodies, peptides, and synthetic polymers, which were chemically linked with active cytotoxic agents through different linkers to form drug conjugates[1]. Although antibody-drug conjugate (ADC), as a classical drug delivery system, is a promising and rapidly developing cancer treatment strategy[2], the slow diffusion rate and poor tumor penetration may limit its effects in solid tumors. And the prolonged time in circulation of ADC leads to prolonged release of the payload in the blood, which leads to potential systemic toxicity[3-4]. Therefore, we hope to use small molecule inhibitors as target modules to construct miniature drug conjugates to deliver payloads to tumor sites. Besides, the slow release of the payload over time allows the drug to be continuously delivered to the tumor, rather than being quickly cleared from the plasma, reducing overall toxicity[5].

The HER tyrosine kinase family consists of four structurally related cellular receptors: epidermal growth factor receptor (EGFR/HER1), human epidermal growth factor receptor 2 (HER2/ErbB2), HER3 (ErbB3), and HER4[6-8]. Overexpression or mutation of EGFR is closely related to malignancy, making it an important and potential target[8-10]. EGFR contains an extracellular ligand-binding domain, a hydrophobic transmembrane domain, and a cytoplasmic tyrosine kinase-containing domain[11-12], and two classes of anti-EGFR drugs are currently on the market: small molecules tyrosine kinase inhibitors (TKIs), which bind to the intracellular catalytic site of EGFR, and monoclonal antibodies (mAbs), which directed against the extracellular domain that prevents receptor dimerization[13-16]. There are many EGFR inhibitors currently in clinical application, such as first-generation Erlotinib and Gefitinib[13], second-generation Afatinib[17], and third-generation Osimertinib[18] (Fig. 1). It has been developed to the fourth generation, such as TQB3804, which has entered clinical phase I trial[19], but these inhibitors are ultimately unable to cross the resistance chasm, limiting its therapeutic application. In addition, severe side effects and tissue toxicity are stumbling blocks to its clinical use[19-20].

The production of nicotinamide adenine dinucleotide (NAD+) is a key biochemical process in mammalian cells and a key component of cellular metabolism[21]. The major NAD biosynthetic pathway in mammals is the conversion of nicotinamide (NAM) and 5'-phosphoribosy-1-pyrophosphate (5-PRPP) to nicotinamide mononucleotide (NMN) by the rate-limiting enzyme, nicotinamide phosphoribosyl transferase (NAMPT)[22-24]. A large number of studies have shown that NAMPT is overexpressed in cancer cells and is closely associated with the occurrence and development of tumors, making it an attractive target for tumor therapy[25-26]. Marketed NAMPT inhibitors include FK866[27] and CHS828[26] (Fig. 1), but their clinical use was limited due to the rapid *in vivo* clearance of FK866 as well as off-target effects and dose-limiting toxicities such as thrombocytopenia and gastrointestinal effects[28-29].

Herein, we envision increasing the in situ concentration of the payload and achieving targeted killing of tumor cells to improve efficacy by utilizing the targeting ability of EGFR inhibitors to deliver the payload into tumor cells. Hybrid monomolecules with both EGFR&HER2 targeting ability and NAMPT enzyme inhibitory activity have great application prospects. In this paper, the EGFR&HER2 inhibitor was chemically connected with the NAMPT inhibitor, and a series of compounds were synthesized and biologically evaluated. Among them, compound **20c** displayed excellent enzyme inhibitory activity and anti-proliferation activity *in vitro*, and could effectively improve the resistance of traditional EGFR inhibitors.

2. Results And Discussion

2.1 Design of EGFR&NAMPT drug conjugates.

Studies have revealed that 4-anilinoquinazoline derivatives with the quinazoline as the core structure are selective and potent EGFR inhibitors[30]. Erlotinib has been reported to bind to the EGFR-binding domain, quinazoline and aniline occupy ATP binding sites and hydrophobic pockets as irreplaceable groups, respectively[31]. The co-crystal structure of Gefitinib and EGFR showed that the side chain at C-6 position of quinazoline protrudes from the surface of the binding pocket[32], which is flexible to tolerate the modification, and this position was selected as the binding site (Fig. 2).

The pharmacophore of NAMPT inhibitors consists of four parts: the pyridine ring of FK866 acting as a NAM mimetic, carbonyl oxygen atoms and amide nitrogen atoms of the spacer mediate the formation of hydrogen bonds, the aliphatic carbon atoms of the linker interacting with the hydrophobic side chain in the domain and the phenyl ring of the inhibitor acting as the solvent-exposed part[33]. The NAMPT binding site exposed to the solvent moiety is tolerant to structural modification[34], so we selected this moiety as the binding site for NAMPT inhibitors in this paper (Fig. 2). As shown in Fig. 2, we chemically combined EGFR&HER2 inhibitors and NAMPT inhibitors to a monomolecular through various linkers to obtain conjugates with EGFR&HER2 inhibitors as targeting ligands.

2.2 Chemistry.

The first-generation EGFR inhibitors Erlotinib and Gefitinib and the EGFR&HER2 dual-target inhibitor Lapatinib were chosen as the main skeletons to construct the drug conjugates of NAMPT and EGFR&HER2 in Schemes 1 ~ 4.

As shown in Scheme 1, the commercially available compound 6-acetoxy-4-chloro-7-methoxyquinazoline was used as the starting material. Chlorine atom at C-4 position underwent an aromatic amine substitution reaction with aniline compounds **2a ~ 2c** to obtain **3a ~ 3c**, followed by deprotection of the acetyl group. The obtained phenolic hydroxy compounds **4a ~ 4c** were alkylated with bromoalkanoates with various lengths to generate **5a ~ 5i**. The carboxyl compounds **6a ~ 6i** after base hydrolysis were condensed with compound **10** and glycine-modified FK866(**11**) under the conditions of EDCI and HOBT to obtain the target product **7a ~ 7f**, **8a ~ 8c** and **9a ~ 9c**.
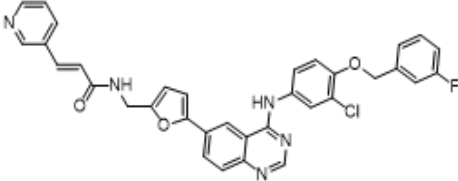
As shown in Scheme 2 and Scheme 3, commercially available compound **12** was selected as the raw material, which was catalyzed by triphenylphosphine palladium dichloride to undergo Suzuki coupling with boronic acid compounds **13** or **14** to generate **15a ~ 15d**. Among them, the aldoximes after the nucleophilic addition of **15a** and **15b** to hydroxylamine hydrochloride could obtain aliphatic amines **17a** and **17b** under the condition of hydrogenation, subsequent condensation with trans-3-(3-pyridyl) acrylic acid (**18**) or amino-substituted 3-(3-pyridyl) acrylic acid (**19**) afforded target compounds **20a ~ 20d**. However, **23a ~ 23c** were directly synthesized by acetylation of compound **10** or **11** with compound **15c** or **15d**.

In Scheme 4, we opted for the direct reductive amination of **15a** with amines under sodium triacetoxyborohydride to prepare **24a ~ 24g**. Finally, compound **18** was conversed to the acid chloride to achieve the final products **25a ~ 25g** with a higher yield.

2.3 Molecular docking analysis

To analyze the binding mode of interactions between **20c** and EGFR, molecular docking model studies were conducted. The results showed that **20c** had a good binding effect with the target protein (binding energy of -7.42 kcal/mol) and a high matching degree, and performed well in protein scoring and binding mode.

Table 1. Target protein docking results for compound **20c**

Target	Compound	Structure	Binding Energy (kcal/mol)	Combination Type
EGFR	20c		-7.42	Hydrogen bonds, Hydrophobic interactive

The complex formed by **20c** and EGFR after docking is visualized using Pymol2.1 software to obtain the binding mode of **20c** and EGFR. According to the binding mode, it can be clearly seen that the amino acids in the active pocket of EGFR protein, such as SER-797, MET-793, and LYS-745 form strong hydrogen bond interactions with **20c**. Moreover, the hydrogen bond distance is relatively short, both of which are far less than 3.5Å. Therefore, **20c** has a strong binding ability with EGFR, making an important contribution to stabilizing small molecules. In addition, combining with Fig. 3B, it can be found that **20c** fits well with the protein pocket, which is conducive to the formation of stable complexes. Importantly, the benzene ring of **20c** can also form a pi-pi conjugate interaction with the benzene ring of the PHE-723 residue. In summary, **20c** binds well to EGFR protein and can form stable complexes.

2.4 *In vitro* EGFR&HER2 and NAMPT inhibition assay

To demonstrate that the modification of compounds still retained inhibitory activity against EGFR&HER2 and NAMPT, we performed *in vitro* enzyme activity assays and selected Afatinib and FK866 as positive controls. As shown in Table 2, when the NAMPT inhibitor FK866 was modified with glycine, the inhibition rate of EGFR enzyme improved slightly with the increase of linker length among compounds **7a ~ 7f**, but there was almost no inhibition of HER2 enzyme. It indicated that glycine modification did not seem to be beneficial to enzyme activity. Notably, compounds **9a ~ 9c** with Lapatinib skeleton as the core structure showed significantly enhanced EGFR&HER2 enzyme inhibitory activity among all conjugates.

Table 2
In vitro EGFR and HER2 inhibitory rate
of the target compounds.

Comps (µM)		Inhibition rate (%)	
		EGFR	HER2
7a	10	55.1	-36.6
	1	16.8	18.6
7b	10	72.9	-19.1
	1	21.6	10.8
7c	10	82.4	9.8
	1	17.9	8.5
7d	10	84.5	10.1
	1	-0.1	-0.7
7e	10	61.6	11.8
	1	6.1	13.4
7f	10	58.8	8.8
	1	10.1	7.9
8a	10	19.0	30.6
	1	4.9	3.3
8b	10	20.3	38.9
	1	13.1	18.5
8c	10	23.7	37.0
	1	13.4	25.2
9a	10	73.1	75.7
	1	69.5	62.9
9b	10	75.0	67.9
	1	64.9	57.9
9c	10	70.5	55.7
	1	69.7	53.4
Afatinib [a]	1	95.7	72.4

Encouraged by previous results, we synthesized conjugates **20a ~ 20d** and **23a ~ 23c** based on the structure of Lapatinib. Table 3 showed that due to the steric effect caused by the longer linker and more carbon atoms, the EGFR&HER2 enzyme activities of compounds **23a ~ 23c** were poor. When only 3-vinyl pyridine (the active part of FK866) was retained, compounds **20a ~ 20d** all exhibited stronger EGFR&HER2 enzyme inhibitory activities. In addition, we also found that C-6 position heterocyclic ring of quinoline skeleton had no obvious effect on EGFR&HER2 activity of conjugates. However, when an amino group was introduced at the 2-position of 3-vinyl pyridine of the NAMPT inhibitor fragment, the inhibitory activity of NAMPT enzyme decreased significantly (Table 2). Among all these compounds, compound **20c** displayed both excellent EGFR&HER2 and NAMPT enzyme inhibitory activities.

Subsequently, compounds **25a ~ 25c** were synthesized based on compound **20c** by introducing different steric hindrance groups to the exposed amino group of 3-vinyl pyridine to analyze whether the substitution has an impact on the activity. It was found that the enzyme activity of EGFR&HER2 increased to low nanomolar levels when small steric groups were introduced, especially for compounds **25a** and **25c**, with IC_{50} values of 7.0 nM and 4.5 nM, respectively. Based on the above results, small steric hindrance groups, such as ethyl, n-propyl, isopropyl, and cyclopropyl were introduced to produce compounds **25d ~ 25g**. Unfortunately, both EGFR&HER2 enzyme and NAMPT enzyme activity of the compounds were decreased, indicating that only methyl modification could be tolerated at this position. Generally speaking, compounds **20c** and **25a** exhibited excellent EGFR&HER2 enzymatic activity and NAMPT enzymatic activity, which could be further characterized biologically.

Table 3
In vitro NAMPT and EGFR inhibitory activities of the target compounds.

Comps	IC$_{50}$ (nM) [a]		
	EGFR	HER2	NAMPT
20a	32.6 ± 2.3	38.4 ± 5.1	1195.5
20b	19.5 ± 2.9	33.7 ± 4.9	341.0
20c	15.6 ± 2.2	25.8 ± 2.1	65.5
20d	26.2 ± 4.6	48.8 ± 6.2	81.5
23a	314.0 ± 66.0	33.9 ± 4.5	NT [b]
23b	1847.1 ± 60.9	7311.4 ± 2602.9	NT
23c	224.0 ± 88.5	95.1 ± 2.2	NT
25a	7.0 ± 0.1	47.9 ± 6.2	54 ± 7
25b	100.7 ± 7.7	2196.1 ± 491.2	361 ± 55
25c	4.5 ± 0.1	42.5 ± 5.6	109 ± 16
25d	49.7 ± 0.8	146.6 ± 30.7	3580 ± 566
25e	86.1 ± 3.2	162.7 ± 26.5	966 ± 188
25f	41.8 ± 6.0	56.3 ± 1.5	1402 ± 66
25g	74.4 ± 12.0	59.3 ± 5.4	280 ± 35
Afatinib [c]	0.4 ± 0.1	13.9 ± 4.8	NT
FK866 [c]	NT	NT	12 ± 4

[a] IC$_{50}$ values represent the mean of at least three independent experiments.

[b] NT = Not tested.

[c] Positive controls.

2.4 *In vitro* antiproliferative inhibition assay

2.4.1 Antiproliferative activities of compounds 20c, 25a and 25c in various cancer cell lines

After screening the conjugates with high activity at the molecular level, six different cancer cell lines were selected and the antiproliferative activity of the compounds were evaluated, and Lapatinib and FK866 were chosen as positive controls. As shown in Table 4, compared with MDA-MB-453 cells with no expression of EGFR&HER2 and MDA-MB-468 and MDA-MB-435 cells with only expression of EGFR or HER2[35], all compounds have excellent anti-proliferative activity in SK-BR-3 and NCI-N87 cells with high expression of EGFR and HER2. Among them, compound **20c** showed better activity than Lapatinib in most cell lines, suggesting that the introduction of a NAMPT payload did enhance the cytotoxicity of the compound, with the expectation of reducing the administration dose of Lapatinib and further avoiding the development of drug resistance. In addition, the cytotoxic activity of compounds **20c** (IC_{50} = 0.36 μM) and **25a** (IC_{50} = 2.5 μM) was better than that of Lapatinib (IC_{50} = 13.5 μM) in the T47D cell line insensitive to Lapatinib[36]. Therefore, we preliminarily infer that it could enhance sensitivity to Lapatinib-resistant cells. Particularly, in the MDA-MB-435 cell line, compound **20c** showed better antiproliferative activity than both positive controls and combined administration, with IC_{50} value of 4.5 μM, which further underlined the role of EGFR inhibitor as a targeting ligand. Importantly, compound **20c** is potential to avoid off-target effects and dose-limiting toxicity that are common with NAMPT inhibitors.

Table 4
Antiproliferative activities of compounds.

Comps	IC_{50} (μM) [a]					
	SK-BR-3	MDA-MB-468	T47D	MDA-MB-453	MDA-MB-435	NCI-N87
20c	0.25 ± 0.05	1.9 ± 0.2	0.36 ± 0.08	1.0 ± 0.1	4.5 ± 0.2	0.15 ± 0.05
25a	0.16 ± 0.02	6.8 ± 1.6	2.5 ± 1.2	5.4 ± 0.03	10.3 ± 1.6	0.11 ± 0.04
25c	0.12 ± 0.03	> 10	> 30	2.1 ± 0.2	> 30	0.07 ± 0.03
FK866 [b]	> 30	6.5 ± 6.8	0.12 ± 0.02	0.99 ± 0.5	> 30	> 30
Lapatinib [b]	0.05 ± 0.004	7.4 ± 4.1	13.5 ± 0.7	1.9 ± 1.6	21.4 ± 8.7	0.03 ± 0.01
FK866+ Lapatinib [c]	0.07 ± 0.04	0.5 ± 0.08	0.17 ± 0.02	0.62 ± 0.3	22.2 ± 5.8	0.03 ± 0.02

[a] IC_{50} values represent the mean of at least three independent experiments (Method A).

[b] Positive controls.

[c] Combined administration.

2.4.2 Antiproliferative activity of compound 20c in Osimertinib-resistant mutant cell lines

It was common knowledge that the first-generation EGFR inhibitors in EGFR-positive patients would develop resistance due to the T790M mutation (the main reason) after continuous administration for 1−2 years, and the third-generation inhibitor Osimertinib (AZD9291) was mainly produced against T790M mutation and had a strong inhibitory effect on L858R/T790M mutation or exon 19 deletion mutation[37−39]. However, once the C797S mutation was produced, the activity of AZD9291 dropped greatly[40]. The NCI-1975 cell carried the L858R/T790M/C797S triple mutation and the Ba/F3 cell had another clinically more common Del19/T790M/C797S triple mutation, and these two Osimertinib-resistant cells were selected for the evaluation of anti-proliferative activity[41−44]. We aimed to demonstrate that our compounds could alleviate the problem of resistance. In Table 5, compound **20c** exhibited 2- to 3-fold higher antiproliferative activity than AZD9291 in both cells with IC_{50} values of 2.15 μM and 0.65 μM, respectively. This result portended that our design strategy was expected to ameliorate the resistance caused by previous EGFR inhibitors, and it was also expected to provide more treatment options for patients who are resistant to Osimertinib after their disease progresses, so as to meet their treatment needs.

Table 5
Antiproliferative activity of compound **20c** in Osimertinib-resistant mutant cell lines.

Comps	IC_{50} (μM) [a]	
	NCI-H1975-EGFR-L858R/T790M/C797S	Ba/F3-EGFR-Del19/T790M/C797S
20c	2.15	0.65
AZD9291[b]	3.93	1.47

[a] IC_{50} values represent the mean of at least three independent experiments (Method B).

[b] Positive control.

2.5 Drug Endocytosis Assay.

In order to analyze whether EGFR inhibitor can act as a target ligand and bring the payload into tumor cells, the drug endocytosis experiment was carried out. Figures 4A and 4B showed that within 4 h of the action time, the drug endocytosis of all compounds in MDA-MB-453 cells (HER2 (-) EGFR (-))[35] and SK-BR-3 cells (HER2 (+) EGFR (+)) [45] was significantly higher than that of the positive control FK866, which was not detected in the cells. It indicated that compounds could take advantage of the targeting ability of EGFR inhibitor to bring the anti-tumor payload into tumor cells, thus exerting therapeutic effect at tumor site. Furthermore, the endocytosis of compound **25c** (the column in green) in both cells was relatively higher than others, that was, the amount of **25c** entering cells per unit time was higher than that of other

compounds, which also explained why **25c** showed the highest EGFR&HER2 enzymatic inhibitory activity. From Fig. 4C to Fig. 4F, the endocytosis of all tested compounds was higher than that in SK-BR-3 cells compared with MDA-MB-453 cells, indicating that these compounds were selective to cells with high expression of EGFR and HER2.

3. Conclusion

We synthesized a series of drug conjugates of EGFR/HER2 inhibitors and NAMPT inhibitors by chemical linkage and *in vitro* pharmacodynamic evaluations were performed. By optimizing the structure of EGFR/HER2 inhibitors and the length of the linker, it was found that modifications of FK866 were redundant for the enzyme inhibitory ability and the linker length was also a critical factor in the activity of the conjugate. Among them, compound **20c** and **25a** have excellent enzyme inhibitory activity and antiproliferative activity *in vitro*. Besides, compound **20c** exhibited superior anti-proliferative activity to Lapatinib in the Lapatinib-resistant cell line T47D, suggesting that our strategy may be a promising therapy for the conundrum of EGFR inhibitor resistance. In NCI-1975 cells with L858R/T790M/C797S triple mutation and Ba/F3 cells with Del19/T790M/C797S triple mutation, both cells were resistant to AZD9291, we found that compound **20c** showed more than 2-fold higher antiproliferative activity than AZD9291, which was definitely the icing on the cake for the proof of concept. By maximizing the fusion of the pharmacophore of the two inhibitors into a single molecule, our compounds are simpler and easier to synthesize. Last but not least, the combination strategy in this paper may be an effective way to ameliorate the severe side effects of EGFR/HER2 inhibitors and NAMPT inhibitors when used alone.

4. Experimental Section

4.1 General Methods. All commercially available solvents and reagents can be used directly without purification, and all reaction progress was monitored by thin-layer chromatography (TLC) under 254nm or 365nm UV light or using appropriate chromogenic reagent. Hydrogen and carbon data recorded by Bruker DRX-400 (400 MHz), CDCl$_3$ and DMSO-d_6 were selected as deuterated solvents, and TMS was used as the internal standard. Purification of all final target compounds was performed with Agilent 1260 series HPLC system using the following conditions: mobile phase A was 0.1% TFA/H$_2$O and mobile phase B was CH$_3$CN. Mobile phase gradient was 95%A for 1 min, 95%A to 5%A for 15 min, 5%A for 2 min, and 5%A to 95%A for 2 min. The flow rate was 1 ml/min and the wavelength was 254 nm. The purity of the final target compounds was >96%.

4.2 General Procedure for the Synthesis of Compounds 7a ~ 7f, 8a ~ 8c and 9a ~ 9c. To a solution of compounds **6a ~ 6i** (0.159 mmol) in anhydrous DMF (3 mL) was added EDCI (45.7 mg, 0.239 mmol), HOBT (32.3 mg 0.239 mmol and synthesized compounds **10 or 11** (63.0 mg, 0.175 mmol). After stirring in an ice bath for half an hour, DIPEA (61.6 mg, 0.477 mmol) was added. The mixture was stirred at room temperature for 4 h. After the reaction completed, the residue was diluted with H$_2$O (30mL) and extracted

with EtOAc (3 × 20 mL). The combined organic layers were then washed with HCl (0.1 M), saturated brine, dried over anhydrous Na_2SO_4, and concentrated in vacuo. The crude product was separated by column chromatography with DCM/MeOH (50:1→25:1) to give **7a ~ 7f, 8a ~ 8c and 9a ~ 9c**.

(E)-N-(4-(1-((2-((4-((3-ethynylphenyl)amino)-7-methoxyquinazolin-6 yl)oxy)acetyl)glycyl)piperidin-4-yl)butyl)-3-(pyridin-3-yl)acrylamide **7a.**

^{1}H NMR (400 MHz, DMSO-d_6) δ 9.47 (s, 1H), 8.75 (s, 1H), 8.54 (d, *J* = 4.6 Hz, 1H), 8.53 (s, 1H), 8.18 (t, *J* = 5.3 Hz, 1H), 8.11 (t, *J* = 5.0 Hz, 1H), 7.97 (d, *J* = 7.5 Hz, 2H), 7.90 (d, *J* = 4.9 Hz, 2H), 7.45 (d, *J* = 7.4 Hz, 1H), 7.43 (d, *J* = 5.4 Hz, 1H), 7.38 (d, *J* = 8.0 Hz, 1H), 7.26 (s, 1H), 7.20 (d, *J* = 7.5 Hz, 1H), 6.72 (d, *J* = 15.9 Hz, 1H), 4.76 (s, 2H), 4.30 (d, *J* = 12.5 Hz, 1H), 4.21 (s, 1H), 4.07 (d, *J* = 4.9 Hz, 2H), 3.98 (s, 3H), 3.78 (d, *J* = 12.5 Hz, 1H), 3.20 − 3.15 (m, 2H), 2.96 (t, *J* = 12.1 Hz, 1H), 2.62 (d, *J* = 36.4 Hz, 1H), 1.64 (d, *J* = 16.1 Hz, 2H), 1.46 − 1.42 (m, 3H), 1.28 (d, *J* = 14.9 Hz, 3H), 1.20 − 1.17 (m, 1H), 1.06 (d, *J* = 12.0 Hz, 1H), 0.92 (d, *J* = 9.5 Hz, 1H). Yield: 53.8 mg, 50.2%. HRMS (ESI) m/z: calcd for $C_{38}H_{41}N_7O_5$ [M + H]$^+$, 676.3247; found, 676.3224. Melting point: 183-184 ℃.

(E)-4-((4-((3-ethynylphenyl)amino)-7-methoxyquinazolin-6-yl)oxy)-N-(2-oxo-2-(4-(4-(3-(pyridin-3-yl)acrylamido)butyl)piperidin-1-yl)ethyl)butanamide **7b.**

^{1}H NMR (400 MHz, DMSO-d_6) δ 9.47 (s, 1H), 8.74 (s, 1H), 8.53 (d, *J* = 4.5 Hz, 1H), 8.50 (s, 1H), 8.18 (s, 1H), 8.11 (s, 1H), 8.03 (s, 1H), 7.97 (d, *J* = 7.9 Hz, 1H), 7.93 (d, *J* = 8.4 Hz, 1H), 7.84 (s, 1H), 7.45 (d, *J* = 6.5 Hz, 1H), 7.42 (s, 1H), 7.38 (d, *J* = 7.9 Hz, 1H), 7.20 (s, 2H), 6.73 (d, *J* = 15.9 Hz, 1H), 4.26 (d, *J* = 12.5 Hz, 1H), 4.18 (d, *J* = 7.3 Hz, 4H), 3.94 (s, 3H), 3.72 (d, *J* = 12.9 Hz, 1H), 3.42 (s, 1H), 3.16 (d, *J* = 6.0 Hz, 2H), 2.86 (s, 1H), 2.46 (s, 1H), 2.41 (s, 2H), 2.09 − 2.04 (m, 2H), 1.60 (s, 2H), 1.41 (d, *J* = 6.8 Hz, 2H), 1.26 (s, 2H), 1.20 (s, 1H), 1.16 (s, 2H), 0.95 (d, *J* = 11.0 Hz, 1H), 0.83 (d, *J* = 11.6 Hz, 1H); ^{13}C NMR (100 MHz, DMSO-d_6) δ 166.78, 165.50, 163.74, 155.64, 153.78, 152.51, 149.45, 148.46, 146.84, 146.56, 139.14, 134.45, 133.27, 130.13, 128.29, 125.80, 124.03, 123.70, 123.36, 121.88, 121.17, 108.12, 106.94, 103.31, 82.86, 80.02, 67.39, 55.45, 43.61, 41.26, 39.72, 38.07, 34.90, 34.51, 31.53, 30.92, 28.66, 22.89. Yield: 53.4 mg, 47.8%. HRMS (ESI) m/z: calcd for $C_{40}H_{45}N_7O_5$ [M + H]$^+$, 704.3560; found, 704.3536. Melting point: 183-184 ℃.

(E)-5-((4-((3-ethynylphenyl)amino)-7-methoxyquinazolin-6-yl)oxy)-N-(2-oxo-2-(4-(4-(3-(pyridin-3-yl)acrylamido)butyl)piperidin-1-yl)ethyl)pentanamide **7c.**

^{1}H NMR (400 MHz, DMSO-d_6) δ 9.88 (s, 1H), 8.73 (s, 1H), 8.53 (d, *J* = 4.3 Hz, 1H), 8.48 (s, 1H), 8.35 (s, 1H), 8.10 (d, *J* = 4.0 Hz, 2H), 8.02 (s, 1H), 8.00 (s, 1H), 7.96 (d, *J* = 7.9 Hz, 1H), 7.45 − 7.41 (m, 2H), 7.37 (s, 1H), 7.18 (s, 2H), 6.82 (d, *J* = 15.9 Hz, 1H), 4.29 (d, *J* = 12.7 Hz, 1H), 4.22 (d, *J* = 6.2 Hz, 2H), 4.18 (s, 1H), 3.93 (s, 3H), 3.90 (s, 1H), 3.74 (d, *J* = 12.7 Hz, 1H), 3.16 (d, *J* = 6.1 Hz, 2H), 2.91 (s, 1H), 2.26 (d, *J* = 6.9 Hz, 2H), 1.84 − 1.80 (m, 2H), 1.72 (d, *J* = 7.1 Hz, 2H), 1.64 (s, 2H), 1.46 − 1.39 (m, 4H), 1.29 (s, 3H), 1.20 (s, 2H), 1.01 (d, *J* = 10.3 Hz, 1H), 0.88 (d, *J* = 10.2 Hz, 1H); ^{13}C NMR (100 MHz, DMSO-d_6) δ 172.01, 166.55, 164.43, 156.12, 154.46, 152.72, 150.08, 149.10, 148.18, 146.94, 139.94, 135.10, 133.93, 130.79, 128.92, 126.30, 124.69, 124.36, 124.00, 122.48, 121.77, 108.93, 107.29, 102.58, 83.59, 80.56, 68.05, 55.88, 44.26,

41.67, 40.54, 38.74, 35.55, 35.18, 32.20, 31.51, 31.38, 29.30, 24.42, 23.54; ^{13}C NMR (100 MHz, DMSO) δ 172.66, 167.03, 164.89, 156.72, 154.89, 153.08, 150.48, 149.52, 148.71, 147.40, 140.53, 135.31, 134.32, 131.28, 129.15, 126.61, 125.30, 125.02, 124.43, 123.17, 122.04, 109.57, 107.61, 103.76, 84.13, 80.91, 69.22, 56.30, 44.72, 42.12, 40.85, 39.15, 36.01, 35.64, 35.20, 32.67, 32.01, 29.72, 28.43, 23.99, 22.54. Yield: 62.5 mg, 54.9%. HRMS (ESI) m/z: calcd for $C_{41}H_{47}N_7O_5$ [M + H]$^+$, 718.3717; found, 718.3700. Melting point: 183-184 °C.

*(E)-N-(4-(1-(2-((4-((3-ethynylphenyl)amino)-7-methoxyquinazolin-6-yl)oxy)acetyl)piperidin-4-yl)butyl)-3-(pyridin-3-yl)acrylamide **7d**.*

^{1}H NMR (400 MHz, CDCl$_3$) δ 8.74 (s, 1H), 8.64 (s, 1H), 8.57 (s, 1H), 8.32 (s, 1H), 7.94 (s, 1H), 7.84 − 7.76 (m, 2H), 7.62 (s, 1H), 7.59 (s, 1H), 7.52 (s, 1H), 7.33 (d, J = 7.9 Hz, 4H), 6.48 (d, J = 15.7 Hz, 1H), 4.46 (s, 1H), 4.17 (d, J = 12.4 Hz, 1H), 4.00 (s, 3H), 3.36 (s, 2H), 3.09 (s, 1H), 3.03 (s, 1H), 2.91 (s, 2H), 1.42 (s, 2H), 1.30 (s, 2H), 1.03 (d, J = 11.9 Hz, 2H), 0.94 (d, J = 6.3 Hz, 2H), 0.91 (s, 1H), 0.87 (s, 2H). ^{13}C NMR (100 MHz, DMSO-d_6) δ 165.32, 164.85, 156.84, 154.87, 153.21, 150.51, 149.56, 147.91, 140.46, 135.44, 134.33, 131.24, 130.13, 129.18, 126.68, 125.19, 124.88, 124.45, 123.09, 122.06, 109.38, 107.52, 104.75, 84.12, 80.98, 67.65, 56.37, 46.85, 36.10, 35.67, 29.75, 27.88, 24.01, 19.84, 14.44, 14.01. Yield: 51.1 mg, 52.1%. HRMS (ESI) m/z: calcd for $C_{36}H_{38}N_6O_4$ [M + Na]$^+$, 641.2852; found, 641.2869. Melting point: 181-182 °C.

*(E)-N-(4-(1-(4-((4-((3-ethynylphenyl)amino)-7-methoxyquinazolin-6-yl)oxy)butanoyl)piperidin-4-yl)butyl)-3-(pyridin-3-yl)acrylamide **7e**.*

^{1}H NMR (400 MHz, CDCl$_3$) δ 8.83 (s, 1H), 8.75 (s, 1H), 8.67 (s, 1H), 8.57 (s, 2H), 8.21 (d, J = 9.0 Hz, 1H), 8.01 (s, 1H), 7.78 (d, J = 7.1 Hz, 1H), 7.62 (d, J = 15.5 Hz, 1H), 7.32 (d, J = 7.6 Hz, 3H), 7.22 (d, J = 10.6 Hz, 2H), 6.45 (d, J = 15.6 Hz, 1H), 4.73 (d, J = 11.5 Hz, 1H), 4.35 − 4.29 (m, 2H), 4.03 (s, 3H), 3.90 (d, J = 13.3 Hz, 1H), 3.43 − 3.38 (m, 2H), 3.08 (s, 1H), 3.03 (d, J = 12.8 Hz, 1H), 2.68 (d, J = 14.3 Hz, 1H), 2.48 (s, 2H), 2.28 (s, 2H), 1.80 (s, 2H), 1.57 − 1.53 (m, 2H), 1.40 (s, 2H), 1.32 (s, 2H), 1.25 (s, 1H), 1.18 − 1.11 (m, 2H); ^{13}C NMR (100 MHz, DMSO-d_6) δ 170.12, 164.84, 156.55, 154.87, 153.14, 150.51, 149.54, 148.67, 147.40, 140.33, 135.52, 134.33, 131.22, 129.32, 126.75, 125.14, 124.80, 124.42, 122.96, 122.19, 109.38, 107.72, 103.05, 84.00, 81.00, 68.64, 56.32, 45.56, 41.87, 39.16, 36.03, 35.74, 32.81, 32.15, 29.75, 28.95, 24.74, 23.99. Yield: 49.2 mg, 48.0%. HRMS (ESI) m/z: calcd for $C_{38}H_{42}N_6O_4$ [M + Na]$^+$, 669.3165; found, 669.3188. Melting point: 184-185 °C.

*(E)-N-(4-(1-(5-((4-((3-ethynylphenyl)amino)-7-methoxyquinazolin-6-yl)oxy)pentanoyl)piperidin-4-yl)butyl)-3-(pyridin-3-yl)acrylamide **7f**.*

^{1}H NMR (400 MHz, CDCl$_3$) δ 9.15 (s, 1H), 8.74 (s, 1H), 8.64 (s, 1H), 8.57 (d, J = 4.6 Hz, 1H), 8.01 (s, 1H), 7.98 (d, J = 8.4 Hz, 1H), 7.78 (s, 2H), 7.61 (d, J = 15.9 Hz, 1H), 7.31 (d, J = 8.5 Hz, 3H), 7.23 (s, 2H), 6.45 (d, J = 15.4 Hz, 1H), 4.41 (s, 3H), 4.01 (s, 3H), 3.83 (d, J = 14.3 Hz, 1H), 3.38 (d, J = 6.9 Hz, 2H), 3.08 (s, 1H), 3.00 (d, J = 11.6 Hz, 1H), 2.57 − 2.53 (m, 2H), 2.42 (t, J = 12.8 Hz, 1H), 1.97 (dd, J = 14.9, 7.3 Hz, 2H), 1.81

(s, 2H), 1.75 (d, J = 13.0 Hz, 1H), 1.54 − 1.50 (m, 3H), 1.33 (d, J = 7.3 Hz, 3H), 1.25 (s, 2H), 1.08 (d, J = 16.5 Hz, 1H), 0.97 (d, J = 13.3 Hz, 1H). ^{13}C NMR (100 MHz, DMSO-d_6) δ = 170.59, 164.88, 156.73, 154.86, 153.05, 150.48, 149.53, 148.68, 147.33, 140.52, 135.31, 134.30, 131.27, 129.14, 126.62, 125.32, 125.00, 124.43, 123.19, 122.03, 109.57, 107.54, 103.74, 84.12, 80.92, 69.32, 56.30, 45.65, 41.71, 36.05, 35.79, 33.00, 32.56, 32.18, 29.73, 28.58, 24.01, 22.19. Yield: 50.5 mg, 48.2%. HRMS (ESI) m/z: calcd for $C_{39}H_{44}N_6O_4$ [M + H] $^+$, 661.3520; found, 661.3485. Melting point: 187-189 °C.

(E)-N-(4-(1-(2-((4-((3-chloro-4-fluorophenyl)amino)-7-methoxyquinazolin-6-yl)oxy)acetyl)piperidin-4-yl)butyl)-3-(pyridin-3-yl)acrylamide **8a.**

^{1}H NMR (400 MHz, CDCl$_3$) δ 8.73 (s, 1H), 8.60 (s, 1H), 8.56 (d, J = 4.7 Hz, 1H), 8.33 (s, 1H), 7.86 (d, J = 6.3 Hz, 1H), 7.78 (d, J = 8.1 Hz, 1H), 7.61 (d, J = 15.6 Hz, 2H), 7.57 (s, 1H), 7.33 − 7.29 (m, 2H), 7.18 (s, 1H), 7.12 (t, J = 8.7 Hz, 1H), 6.47 (d, J = 15.7 Hz, 1H), 4.94 (s, 2H), 4.47 (d, J = 12.7 Hz, 1H), 4.14 (d, J = 12.9 Hz, 1H), 3.96 (s, 3H), 3.37 (d, J = 6.4 Hz, 2H), 3.05 (s, 1H), 2.58 (t, J = 12.3 Hz, 1H), 1.66 (s, 2H), 1.56 − 1.51 (m, 2H), 1.51 − 1.47 (m, 1H), 1.31 (s, 2H), 1.10 − 0.98 (m, 2H), 0.95 (d, J = 12.5 Hz, 2H); ^{13}C NMR (100 MHz, DMSO-d_6) δ 165.20, 164.84, 156.59, 154.97, 153.31, 150.52, 149.54, 147.93, 147.67, 135.53, 134.34, 131.21, 124.80, 124.43, 123.76, 122.68, 119.33, 119.15, 117.08, 116.87, 109.19, 107.85, 104.10, 67.61, 56.38, 45.31, 42.15, 39.17, 36.08, 35.65, 32.79, 32.12, 29.76, 23.98; ^{13}C NMR (100 MHz, DMSO) δ 165.20, 164.84, 156.59, 154.97, 153.31, 150.52, 149.54, 147.93, 147.67, 135.53, 134.34, 131.21, 124.80, 124.43, 123.76, 122.68, 119.33, 119.15, 117.08, 116.87, 109.19, 107.85, 104.10, 67.61, 56.38, 45.31, 42.15, 39.17, 36.08, 35.65, 32.79, 32.12, 29.76, 23.98. Yield: 54.3 mg, 53.0%. HRMS (ESI) m/z: calcd for $C_{34}H_{36}ClFN_6O_4$ [M + H] $^+$, 647.3346; found, 647.3281. Melting point: 140-141 °C.

(E)-N-(4-(1-(4-((4-((3-chloro-4-fluorophenyl)amino)-7-methoxyquinazolin-6-yl)oxy)butanoyl)piperidin-4-yl)butyl)-3-(pyridin-3-yl)acrylamide **8b.**

^{1}H NMR (400 MHz, CDCl$_3$) δ 8.84 (s, 1H), 8.75 (s, 1H), 8.66 (s, 1H), 8.57 (d, J = 4.5 Hz, 1H), 8.54 (s, 1H), 8.06 (s, 1H), 8.01 (d, J = 6.2 Hz, 1H), 7.79 (d, J = 7.8 Hz, 1H), 7.62 (d, J = 15.8 Hz, 1H), 7.33 (s, 2H), 7.23 (s, 1H), 7.14 (s, 1H), 6.45 (d, J = 15.7 Hz, 1H), 4.69 (d, J = 12.2 Hz, 1H), 4.31 (s, 2H), 4.03 (s, 3H), 3.91 (d, J = 13.2 Hz, 1H), 3.41 (d, J = 6.6 Hz, 2H), 3.06 (s, 1H), 2.67 (s, 1H), 2.49 (s, 2H), 2.27 (s, 2H), 1.81 (d, J = 12.4 Hz, 2H), 1.41 (s, 2H), 1.33 (s, 2H), 1.21 − 1.18 (m, 1H), 1.15 (d, J = 13.2 Hz, 2H), 0.88 (s, 2H); ^{13}C NMR (100 MHz, DMSO-d_6) δ 170.10, 164.83, 156.47, 154.92, 153.07, 150.52, 149.54, 148.70, 147.38, 137.35, 135.51, 134.34, 131.21, 124.79, 124.44, 123.83, 122.72, 122.66, 117.06, 116.85, 109.27, 107.72, 103.04, 68.66, 56.34, 45.57, 41.85, 39.14, 36.03, 35.73, 32.83, 32.16, 29.74, 28.96, 24.79, 23.97. Yield: 50.6 mg, 47.3%. HRMS (ESI) m/z: calcd for $C_{36}H_{40}ClFN_6O_4$ [M + H] $^+$, 675.2862; found, 675.2897. Melting point: 142-144 °C.

(E)-N-(4-(1-(5-((4-((3-chloro-4-fluorophenyl)amino)-7-methoxyquinazolin-6-yl)oxy)pentanoyl)piperidin-4-yl)butyl)-3-(pyridin-3-yl)acrylamide **8c.**

^{1}H NMR (400 MHz, CDCl$_3$) δ 9.25 (s, 1H), 8.74 (s, 1H), 8.63 (s, 1H), 8.57 (d, *J* = 4.7 Hz, 1H), 8.03 (d, *J* = 5.0 Hz, 1H), 7.85 (d, *J* = 8.7 Hz, 1H), 7.78 (s, 2H), 7.61 (d, *J* = 15.7 Hz, 1H), 7.31 (s, 2H), 7.22 (s, 1H), 7.12 (s, 1H), 6.45 (d, *J* = 15.6 Hz, 1H), 4.41 (s, 2H), 4.01 (s, 3H), 3.84 (d, *J* = 13.5 Hz, 1H), 3.38 (d, *J* = 6.5 Hz, 2H), 3.03 (s, 1H), 2.56 (s, 2H), 2.43 (s, 1H), 1.95 (s, 2H), 1.80 (d, *J* = 7.3 Hz, 2H), 1.75 (s, 1H), 1.55 (s, 2H), 1.45 (s, 2H), 1.36 − 1.30 (m, 3H), 1.09 (d, *J* = 11.7 Hz, 2H), 0.98 − 0.89 (m, 2H); ^{13}C NMR (100 MHz, DMSO-d_6) δ 170.52, 164.82, 156.47, 154.94, 153.05, 150.52, 149.55, 148.77, 147.39, 137.35, 135.52, 134.34, 131.21, 124.78, 124.43, 123.89, 122.79, 122.72, 117.08, 116.86, 109.28, 107.71, 102.92, 69.08, 56.34, 45.62, 41.72, 39.15, 36.06, 35.80, 33.00, 32.54, 32.18, 29.75, 28.56, 24.00, 22.16. Yield: 54.6 mg, 50.0%. HRMS (ESI) m/z: calcd for C$_{37}$H$_{42}$ClFN$_6$O$_4$ [M + H] $^+$, 689.3018; found, 689.2990. Melting point: 148-149 °C.

(E)-N-(4-(1-(2-((4-((3-chloro-4-((3-fluorobenzyl)oxy)phenyl)amino)-7-methoxyquinazolin-6-yl)oxy)acetyl)piperidin-4-yl)butyl)-3-(pyridin-3-yl)acrylamide **9a.**

^{1}H NMR (400 MHz, CDCl$_3$) δ 8.73 (s, 1H), 8.59 (s, 1H), 8.56 (d, *J* = 4.7 Hz, 1H), 8.10 (s, 1H), 7.77 (s, 2H), 7.61 (d, *J* = 16.0 Hz, 1H), 7.53 (d, *J* = 10.5 Hz, 2H), 7.38 − 7.35 (m, 1H), 7.31 (d, *J* = 7.4 Hz, 2H), 7.21 (d, *J* = 12.1 Hz, 3H), 7.04 − 7.00 (m, 1H), 6.94 (d, *J* = 8.6 Hz, 1H), 6.47 (d, *J* = 15.9 Hz, 1H), 5.15 (s, 2H), 4.93 (s, 2H), 4.47 (d, *J* = 12.7 Hz, 1H), 4.16 (d, *J* = 14.4 Hz, 1H), 3.97 (s, 3H), 3.35 (s, 2H), 3.04 (s, 1H), 2.58 (t, *J* = 12.2 Hz, 1H), 1.52 (d, *J* = 7.0 Hz, 3H), 1.28 (s, 2H), 1.24 − 1.20 (m, 2H), 1.03 (d, *J* = 12.7 Hz, 2H), 0.95 (d, *J* = 11.5 Hz, 2H); ^{13}C NMR (100 MHz, DMSO-d_6) δ 164.98, 164.61, 163.64, 161.22, 156.53, 154.60, 153.27, 150.29, 149.61, 149.32, 147.59, 147.30, 139.96, 135.30, 134.11, 130.98, 130.84, 124.55, 124.20, 123.60, 122.34, 121.25, 115.04, 114.83, 114.53, 114.40, 114.18, 108.83, 107.60, 103.83, 69.60, 67.35, 56.12, 45.08, 41.92, 35.86, 35.43, 32.56, 31.87, 29.53, 23.75. Yield: 69.4 mg, 49.0%. HRMS (ESI) m/z: calcd for C$_{44}$H$_{42}$F$_3$N$_7$O$_9$ [M + H] $^+$, 753.2967; found, 753.2926. Melting point: 163-165 °C.

(E)-N-(4-(1-(4-((4-((3-chloro-4-((3-fluorobenzyl)oxy)phenyl)amino)-7-methoxyquinazolin-6-yl)oxy)butanoyl)piperidin-4-yl)butyl)-3-(pyridin-3-yl)acrylamide **9b.**

^{1}H NMR (400 MHz, CDCl$_3$) δ 8.79 (d, *J* = 11.3 Hz, 1H), 8.73 (s, 1H), 8.62 (s, 1H), 8.55 (d, *J* = 4.6 Hz, 1H), 8.52 (s, 1H), 8.08 (t, *J* = 10.2 Hz, 1H), 7.85 (s, 1H), 7.77 (d, *J* = 7.9 Hz, 1H), 7.61 (d, *J* = 15.6 Hz, 1H), 7.38 − 7.34 (m, 1H), 7.32 − 7.27 (m, 2H), 7.24 (s, 1H), 7.21 (s, 2H), 7.02 (d, *J* = 8.1 Hz, 1H), 6.97 (d, *J* = 9.1 Hz, 1H), 6.46 (d, *J* = 15.7 Hz, 1H), 5.14 (s, 2H), 4.69 (d, *J* = 13.4 Hz, 1H), 4.29 (d, *J* = 7.3 Hz, 2H), 4.01 (s, 3H), 3.89 (d, *J* = 13.1 Hz, 1H), 3.40 (dd, *J* = 13.2, 6.5 Hz, 2H), 3.09 (s, 2H), 2.65 (t, *J* = 12.5 Hz, 1H), 2.47 (s, 1H), 2.29 (d, *J* = 4.7 Hz, 1H), 2.24 − 2.18 (m, 1H), 1.79 (d, *J* = 13.0 Hz, 2H), 1.60 − 1.55 (m, 2H), 1.39 (s, 2H), 1.30 (d, *J* = 7.3 Hz, 2H), 1.25 (s, 1H), 1.13 (s, 1H), 0.86 (d, *J* = 7.0 Hz, 1H); ^{13}C NMR (100 MHz, DMSO-d_6) δ 170.13, 164.83, 156.67, 154.82, 153.28, 150.52, 149.85, 149.52, 148.61, 147.28, 135.51, 134.35, 134.06, 131.23, 131.07, 124.83, 124.43, 124.36, 123.83, 122.54, 121.52, 115.26, 115.06, 114.83, 114.63, 114.41, 109.21, 107.77, 103.12, 69.91, 68.66, 56.33, 45.58, 41.87, 39.15, 36.02, 35.73, 32.83, 32.16, 29.74, 28.97, 24.82, 23.97. Yield: 64.0 mg, 45.2%. HRMS (ESI) m/z: calcd for C$_{44}$H$_{42}$F$_3$N$_7$O$_9$ [M + H] $^+$, 781.3821; found, 781.3265. Melting point: 160-161 °C.

(E)-N-(4-(1-(5-((4-((3-chloro-4-((3-fluorobenzyl)oxy)phenyl)amino)-7-methoxyquinazolin-6-yl)oxy)pentanoyl)piperidin-4-yl)butyl)-3-(pyridin-3-yl)acrylamide **9c.**

^{1}H NMR (400 MHz, DMSO-d_6) δ 9.48 (s, 1H), 8.74 (s, 1H), 8.55 − 8.53 (m, 1H), 8.44 (s, 1H), 8.31 (s, 1H), 8.16 (t, *J* = 5.4 Hz, 1H), 7.97 − 7.95 (m, 2H), 7.83 (s, 1H), 7.72 (dd, *J* = 8.9, 2.4 Hz, 1H), 7.46 (s, 1H), 7.42 (d, *J* = 3.4 Hz, 1H), 7.33 (d, *J* = 7.5 Hz, 2H), 7.25 (d, *J* = 9.0 Hz, 1H), 7.19 − 7.15 (m, 2H), 6.73 (d, *J* = 15.9 Hz, 1H), 5.24 (s, 2H), 4.37 (d, *J* = 13.0 Hz, 1H), 4.16 (t, *J* = 6.1 Hz, 2H), 3.92 (s, 3H), 3.85 (d, *J* = 13.0 Hz, 1H), 3.17 (d, *J* = 5.9 Hz, 2H), 2.94 (s, 1H), 2.46 (s, 1H), 2.40 (t, *J* = 7.4 Hz, 2H), 1.83 (d, *J* = 7.2 Hz, 2H), 1.72 − 1.68 (m, 2H), 1.64 (s, 1H), 1.43 (d, *J* = 7.0 Hz, 2H), 1.29 (s, 2H), 1.21 − 1.17 (m, 2H), 1.04 − 0.97 (m, 1H), 0.88 (d, *J* = 9.2 Hz, 1H); ^{13}C NMR (100 MHz, DMSO-d_6) δ 170.05, 164.36, 163.40, 160.98, 156.18, 154.33, 152.75, 150.01, 149.35, 149.03, 148.17, 146.77, 139.73, 135.02, 133.85, 133.60, 130.74, 130.56, 124.34, 123.92, 123.31, 122.10, 121.02, 114.76, 114.55, 114.30, 114.12, 113.90, 108.75, 107.22, 102.55, 69.42, 68.60, 55.81, 45.15, 41.24, 35.32, 32.52, 32.08, 31.69, 29.27, 28.10, 23.52, 21.69. Yield: 70.2 mg, 49.6%. HRMS (ESI) m/z: calcd for $C_{44}H_{42}F_3N_7O_9$ [M + H]$^+$, 795.3437; found, 795.3385. Melting point: 158-159 °C.

General Procedure for the Synthesis of Compounds 20a ~ 20d. To a solution of compounds (**17a ~ 17b**, 0.265 mmol) in anhydrous DMAC (5 mL) was added EDCI (203 mg 1.059 mmol), HOBT (143 mg 1.059 mmol) and synthesized compounds **18 or 19** (0.529 mmol). After stirring in an ice bath for half an hour, DIPEA (136.8 mg 1.059 mmol) was added. The mixture was kept at room temperature for 4 h. After the reaction completed, the residue was diluted with H_2O (50mL) and extracted with EtOAc (3 × 30 mL). The combined organic layers were then washed with HCl (0.1 M), saturated brine, dried over anhydrous Na_2SO_4, and concentrated in vacuo to afford the crude product, which was purified by column chromatography with DCM/MeOH (50:1−25:1) to give compounds **20a ~ 20d**.

(E)-3-(6-aminopyridin-3-yl)-N-((5-(4-((3-chloro-4-((3-fluorobenzyl)oxy)phenyl)amino)quinazolin-6-yl)furan-2-yl)methyl)acrylamide **20a.**

^{1}H NMR (400 MHz, v) δ 9.98 (s, 1H), 8.79 (s, 1H), 8.55 (s, 1H), 8.51 (s, 1H), 8.15 (d, *J* = 8.5 Hz, 1H), 8.08 (s, 1H), 8.04 (s, 1H), 7.80 (d, *J* = 8.7 Hz, 1H), 7.76 (d, *J* = 8.4 Hz, 1H), 7.60 (d, *J* = 7.6 Hz, 1H), 7.47 (d, *J* = 6.3 Hz, 1H), 7.36 (d, *J* = 7.0 Hz, 1H), 7.33 (s, 1H), 7.31 − 7.27 (m, 2H), 7.18 (s, 1H), 7.07 (s, 1H), 6.47 (d, *J* = 8.4 Hz, 2H), 6.41 (s, 2H), 5.26 (s, 2H), 4.51 (d, *J* = 4.9 Hz, 2H); ^{13}C NMR (100 MHz, DMSO-d_6) δ 165.94, 161.03, 158.08, 154.76, 153.68, 152.12, 150.25, 150.08, 149.38, 140.18, 137.58, 135.06, 133.57, 131.09, 130.12, 128.98, 128.70, 124.82, 123.84, 123.02, 121.50, 119.43, 117.09, 115.85, 115.28, 115.07, 114.78, 114.63, 114.42, 110.08, 108.76, 108.50, 69.89, 36.48. Yield: 78.9 mg, 48.1%. HRMS (ESI) m/z: calcd for $C_{34}H_{26}ClFN_6O_3$ [M + H]$^+$, 620.1817; found, 621.1810. Melting point: 157-158 °C.

(E)-3-(6-aminopyridin-3-yl)-N-((5-(4-((3-chloro-4-((3-fluorobenzyl)oxy)phenyl)amino)quinazolin-6-yl)thiophen-2-yl)methyl)acrylamide **20b.**

^{1}H NMR (400 MHz, DMSO-d_6) δ 9.97 (s, 1H), 8.67 (s, 1H), 8.65 (d, J = 6.0 Hz, 1H), 8.53 (s, 1H), 8.11 (d, J = 9.2 Hz, 1H), 8.08 (s, 1H), 7.99 (s, 1H), 7.77 (d, J = 8.7 Hz, 1H), 7.71 (d, J = 8.1 Hz, 1H), 7.61 (d, J = 7.3 Hz, 1H), 7.56 (d, J = 3.3 Hz, 1H), 7.47 (d, J = 6.7 Hz, 1H), 7.38 − 7.32 (m, 3H), 7.28 (d, J = 9.1 Hz, 1H), 7.19 (d, J = 7.7 Hz, 1H), 7.08 (d, J = 3.0 Hz, 1H), 6.48 (d, J = 8.8 Hz, 1H), 6.39 (d, J = 19.1 Hz, 3H), 5.26 (s, 2H), 4.60 (d, J = 5.4 Hz, 2H); ^{13}C NMR (100 MHz, DMSO-d_6) δ 165.88, 163.88, 161.46, 161.06, 158.00, 154.79, 150.27, 149.41, 144.26, 141.92, 140.16, 140.09, 137.73, 135.04, 133.44, 132.43, 131.10, 129.07, 127.24, 124.97, 123.85, 123.17, 121.44, 119.35, 118.64, 116.93, 115.83, 115.30, 115.09, 114.70, 114.43, 108.78, 69.81, 38.07. Yield: 87.1 mg, 51.8%. HRMS (ESI) m/z: calcd for $C_{34}H_{26}ClFN_6O_2S$ [M + H] +, 637.1589; found, 637.1578. Melting point: 160-161 °C.

(E)-N-((5-(4-((3-chloro-4-((3-fluorobenzyl)oxy)phenyl)amino)quinazolin-6-yl)furan-2-yl)methyl)-3-(pyridin-3-yl)acrylamide **20c**. ^{1}H NMR (400 MHz, DMSO-d_6) δ 10.90 (s, 1H), 8.82 (d, J = 24.7 Hz, 4H), 8.58 (d, J = 4.6 Hz, 1H), 8.31 (d, J = 8.2 Hz, 1H), 8.03 (d, J = 7.8 Hz, 1H), 7.93 (s, 1H), 7.87 (d, J = 8.9 Hz, 1H), 7.66 (d, J = 8.7 Hz, 1H), 7.53 (s, 1H), 7.48 (d, J = 6.0 Hz, 2H), 7.33 (t, J = 8.1 Hz, 3H), 7.20 (t, J = 8.7 Hz, 1H), 7.13 (d, J = 2.5 Hz, 1H), 6.83 (d, J = 16.1 Hz, 1H), 6.56 (s, 1H), 5.30 (s, 2H), 4.56 (d, J = 5.1 Hz, 2H). ^{13}C NMR (100 MHz, DMSO-d_6) δ 165.01, 163.89, 161.47, 159.32, 153.99, 151.64, 151.43, 150.35, 149.28, 139.97, 139.90, 136.35, 134.88, 131.23, 131.13, 131.05, 130.05, 126.23, 124.63, 124.44, 124.33, 123.84, 121.68, 117.56, 115.36, 115.15, 115.00, 114.75, 114.66, 114.44, 110.50, 109.51, 69.88, 36.58. Yield: 83.2 mg, 52.5%. HRMS (ESI) m/z: calcd for $C_{34}H_{25}ClFN_5O_3$ [M + H] $^+$, 606.1708; found, 606.1674. Melting point: 157-158 °C.

(E)-N-((5-(4-((3-chloro-4-((3-fluorobenzyl)oxy)phenyl)amino)quinazolin-6-yl)thiophen-2-yl)methyl)-3-(pyridin-3-yl)acrylamide **20d**.

^{1}H NMR (400 MHz, DMSO-d_6) δ 9.97 (s, 1H), 8.91 (t, J = 5.7 Hz, 1H), 8.78 (s, 1H), 8.70 (s, 1H), 8.56 (d, J = 4.7 Hz, 1H), 8.54 (s, 1H), 8.12 (d, J = 8.7 Hz, 1H), 8.00 (t, J = 5.7 Hz, 2H), 7.78 (d, J = 8.7 Hz, 1H), 7.72 (dd, J = 8.9, 2.4 Hz, 1H), 7.59 − 7.57 (m, 1H), 7.53 (t, J = 10.1 Hz, 1H), 7.47 (d, J = 5.8 Hz, 1H), 7.46 − 7.43 (m, 1H), 7.33 (d, J = 7.3 Hz, 1H), 7.30 (s, 1H), 7.28 (d, J = 9.0 Hz, 1H), 7.17 (d, J = 7.9 Hz, 1H), 7.12 − 7.09 (m, 1H), 6.80 (d, J = 15.9 Hz, 1H), 5.26 (s, 2H), 4.63 (d, J = 5.7 Hz, 2H). ^{13}C NMR (100 MHz, DMSO-d_6) δ 165.14, 164.98, 163.89, 159.12, 150.53, 149.46, 144.53, 141.27, 139.99, 138.28, 136.55, 134.74, 133.73, 131.13, 131.05, 127.64, 126.16, 125.46, 124.58, 124.37, 124.20, 123.86, 123.84, 121.66, 119.21, 117.19, 115.36, 115.15, 115.09, 114.76, 114.66, 114.44, 69.89, 38.18. Yield: 82.6 mg, 52.1%. HRMS (ESI) m/z: calcd for $C_{34}H_{25}ClFN_5O_2S$ [M + H] $^+$, 622.1487; found, 622.1480. Melting point: 160-161 °C.

General Procedure for the Synthesis of Compounds 23a ~ 23c. To a solution of compounds (**15c ~ 15d**, 0.179 mmol) in anhydrous DMAC (5 mL) was added NMI (73.7 mg 0.898 mmol), and synthesized compounds **10** or **11** (0.216 mmol). Then added TCFH (60.6 mg 0.216 mmol). The mixture was maintained at room temperature for 4 h. After the reaction completed, the residue was diluted with H_2O (50mL) and extracted with EtOAc (3 × 30 mL). The combined organic layers were then washed with

saturated brine, dried over anhydrous Na$_2$SO$_4$, and concentrated in vacuo. The crude product was separated by column chromatography with DCM/MeOH (50:1→25:1) to give compounds **23a ~ 23c**.

(E)-N-(4-(1-(5-(4-((3-chloro-4-((3-fluorobenzyl)oxy)phenyl)amino)quinazolin-6-yl)furan-2-carbonyl)piperidin-4-yl)butyl)-3-(pyridin-3-yl)acrylamide **23a**.

^{1}H NMR (400 MHz, DMSO-d_6) δ 10.04 (s, 1H), 8.84 (s, 1H), 8.74 (s, 1H), 8.59 (s, 1H), 8.54 (d, J = 3.7 Hz, 1H), 8.22 (d, J = 8.7 Hz, 1H), 8.15 (t, J = 5.5 Hz, 1H), 8.00 (d, J = 2.3 Hz, 1H), 7.96 (d, J = 8.0 Hz, 1H), 7.85 (d, J = 8.7 Hz, 1H), 7.72 (dd, J = 8.9, 2.3 Hz, 1H), 7.46 − 7.42 (m, 2H), 7.33 (d, J = 7.5 Hz, 2H), 7.29 (d, J = 9.0 Hz, 2H), 7.23 (d, J = 3.5 Hz, 1H), 7.19 (d, J = 7.0 Hz, 1H), 7.12 (d, J = 3.5 Hz, 1H), 6.72 (d, J = 15.9 Hz, 1H), 5.27 (s, 2H), 4.37 (d, J = 11.1 Hz, 2H), 3.18 (dd, J = 12.6, 6.5 Hz, 4H), 1.78 (d, J = 11.4 Hz, 2H), 1.57 (s, 1H), 1.48 − 1.44 (m, 2H), 1.33 (s, 2H), 1.29 (d, J = 5.7 Hz, 2H), 1.15 (d, J = 10.4 Hz, 2H); ^{13}C NMR (100 MHz, DMSO-d_6) δ 164.83, 163.88, 161.46, 158.68, 158.19, 155.10, 153.73, 150.50, 150.38, 149.52, 147.53, 140.13, 140.05, 135.55, 134.35, 133.33, 131.21, 131.08, 131.00, 129.48, 128.88, 127.80, 124.88, 124.77, 124.43, 123.82, 123.05, 121.53, 118.49, 117.49, 115.75, 115.28, 115.08, 114.72, 114.63, 114.41, 108.68, 69.84, 39.18, 36.00, 35.86, 29.77, 24.02. Yield: 74.0 mg, 54.3%. HRMS (ESI) m/z: calcd for C$_{43}$H$_{40}$ClFN$_6$O$_4$ [M + H]$^+$, 759.2862; found, 759.2799. Melting point: 168-169 °C.

(E)-N-(4-(1-(5-(4-((3-chloro-4-((3-fluorobenzyl)oxy)phenyl)amino)quinazolin-6-yl)thiophene-2-carbonyl)piperidin-4-yl)butyl)-3-(pyridin-3-yl)acrylamide **23b**.

^{1}H NMR (400 MHz, DMSO-d_6) δ 10.18 (s, 1H), 8.81 (s, 1H), 8.76 (d, J = 1.8 Hz, 1H), 8.63 (s, 1H), 8.55 (dd, J = 4.7, 1.4 Hz, 1H), 8.23 (dd, J = 8.7, 1.7 Hz, 1H), 8.16 (t, J = 5.6 Hz, 1H), 7.99 − 7.96 (m, 2H), 7.83 (d, J = 8.7 Hz, 1H), 7.71 (dd, J = 8.9, 2.5 Hz, 1H), 7.68 (d, J = 3.8 Hz, 1H), 7.51 − 7.48 (m, 1H), 7.47 − 7.43 (m, 3H), 7.35 (s, 1H), 7.32 (s, 1H), 7.31 (d, J = 4.1 Hz, 1H), 7.19 (d, J = 2.0 Hz, 1H), 6.73 (d, J = 15.9 Hz, 1H), 5.28 (s, 2H), 4.32 (d, J = 10.8 Hz, 2H), 3.20 (d, J = 6.1 Hz, 2H), 3.01 (s, 2H), 1.77 (d, J = 11.8 Hz, 2H), 1.56 (s, 1H), 1.50 − 1.45 (m, 2H), 1.34 (s, 2H), 1.29 (d, J = 5.3 Hz, 2H), 1.19 − 1.11 (m, 2H); ^{13}C NMR (100 MHz, DMSO-d_6) δ 164.85, 162.03, 158.33, 158.25, 154.63, 150.68, 150.46, 149.47, 145.34, 140.03, 138.38, 135.54, 134.43, 132.87, 131.79, 131.49, 131.24, 131.10, 131.01, 130.47, 127.98, 125.28, 125.16, 124.80, 124.47, 123.82, 123.47, 121.55, 121.44, 119.93, 115.56, 115.31, 115.10, 114.70, 114.63, 114.41, 69.83, 39.17, 35.97, 35.79, 32.60, 29.76, 24.01. Yield: 71.9 mg, 52.0%. HRMS (ESI) m/z: calcd for C$_{43}$H$_{40}$ClFN$_6$O$_3$S [M + H]$^+$, 775.2633; found, 775.2639. Melting point: 170-172 °C.

(E)-N-(2-(5-(4-((3-chloro-4-((3-fluorobenzyl)oxy)phenyl)amino)quinazolin-6-yl)thiophen-2-yl)-2-oxoethyl)-4-(4-(3-(pyridin-3-yl)acrylamido)butyl)piperidine-1-carboxamide **23c**.

^{1}H NMR (400 MHz, DMSO-d_6) δ 9.98 (s, 1H), 8.81 (s, 1H), 8.75 (d, J = 1.9 Hz, 1H), 8.68 (s, 1H), 8.57 (s, 1H), 8.54 (dd, J = 4.7, 1.5 Hz, 1H), 8.22 (dd, J = 8.8, 1.7 Hz, 1H), 8.15 (t, J = 5.5 Hz, 1H), 7.99 (d, J = 2.6 Hz, 1H), 7.97 (d, J = 8.0 Hz, 1H), 7.89 (d, J = 4.0 Hz, 1H), 7.82 (d, J = 8.7 Hz, 1H), 7.75 − 7.71 (m, 2H), 7.47 (d, J = 7.5 Hz, 1H), 7.46 − 7.43 (m, 1H), 7.43 (d, J = 3.3 Hz, 1H), 7.32 (dd, J = 17.4, 8.3 Hz, 3H), 7.18 (d, J = 2.0 Hz, 1H), 6.73 (d, J = 15.9 Hz, 1H), 5.27 (s, 2H), 4.35 (d, J = 12.7 Hz, 1H), 4.13 (d, J = 5.6 Hz, 2H), 3.87 (d, J =

13.5 Hz, 1H), 3.21 − 3.16 (m, 2H), 3.01 (t, J = 12.0 Hz, 1H), 2.57 (s, 1H), 1.70 (t, J = 11.7 Hz, 2H), 1.51 − 1.43 (m, 3H), 1.31 (d, J = 14.7 Hz, 2H), 1.25 (s, 2H), 1.10 − 0.90 (m, 2H); ^{13}C NMR (100 MHz, DMSO-d_6) δ 166.34, 164.31, 163.37, 161.02, 157.57, 154.75, 150.03, 149.84, 149.45, 149.04, 146.51, 139.52, 135.04, 133.84, 132.78, 131.04, 130.69, 130.59, 130.51, 129.24, 128.71, 125.39, 124.49, 124.25, 123.94, 123.34, 122.68, 120.95, 119.33, 115.27, 114.79, 114.58, 114.18, 113.92, 69.29, 44.27, 41.74, 40.73, 38.64, 35.56, 35.17, 32.31, 31.59, 29.25, 23.47. Yield: 76.2 mg, 51.3%. HRMS (ESI) m/z: calcd for $C_{45}H_{43}ClFN_7O_4S$ [M + H] $^+$, 832.2848; found, 832.2865. Melting point: 158-159 °C.

General Procedure for the Synthesis of Compounds 25a ~ 25g. Under nitrogen protection, commercially available 3-(3-pyridyl)-acrylic acid (15.04 mg, 0.101 mmol) was dissolved in anhydrous DCM (2 mL), oxalyl chloride (15.99 mg, 0.126 mmol) was added dropwise under an ice water bath, followed by a catalytic amount of DMF, the mixture was stirred at room temperature for 1 h. After the reaction of the raw materials was completed, the solvent was removed under reduced pressure, and then added dropwise into the anhydrous DCM solution of compounds **24a ~ 24g** (50 mg, 0.084 mmol) and DIPEA (21.72 mg, 0.168 mmol), and reacted at room temperature for 6 h. After the reaction completed, the residue was diluted with H_2O (20mL) and extracted with DCM (3 × 10 mL). The combined organic layers were then washed with saturated brine, dried over anhydrous Na_2SO_4, and concentrated in vacuo to afford the crude product, which was purified by column chromatography with DCM/MeOH (50:1→30:1) to give compounds **25a ~ 25g**.

*(E)-N-((5-(4-((3-chloro-4-((3-fluorobenzyl)oxy)phenyl)amino)quinazolin-6-yl)furan-2-yl)methyl)-N-methyl-3-(pyridin-3-yl)acrylamide **25a**.*

^{1}H NMR (400 MHz, DMSO-d_6) δ 9.90 (d, J = 21.1 Hz, 1H), 8.91 (d, J = 8.9 Hz, 1H), 8.73 (s, 1H), 8.55 (s, 2H), 8.24 − 8.18 (m, 1H), 8.15 − 8.04 (m, 1H), 8.00 (s, 1H), 7.75 (d, J = 32.8 Hz, 2H), 7.59 (s, 1H), 7.47 (d, J = 7.3 Hz, 1H), 7.42 (s, 1H), 7.35 − 7.25 (m, 4H), 7.20 (d, J = 8.7 Hz, 1H), 7.07 (s, 1H), 6.57 (d, J = 21.8 Hz, 1H), 5.26 (s, 2H), 4.85 (d, J = 71.9 Hz, 2H), 3.17 (d, J = 86.2 Hz, 3H). ^{13}C NMR (100 MHz, DMSO-d_6) δ 166.06, 163.89, 161.47, 158.08, 154.80, 152.45, 150.73, 150.29, 150.06, 149.35, 140.16, 140.09, 138.94, 135.01, 133.48, 131.37, 131.09, 131.01, 124.88, 124.79, 124.27, 123.84, 123.09, 121.54, 120.99, 117.31, 115.81, 115.29, 115.08, 114.80, 114.63, 114.42, 69.88, 35.60, 34.54. Yield: 48.2 mg, 57.2%. HRMS (ESI) m/z: calcd for $C_{35}H_{27}ClFN_5O_3$ [M + H] $^+$, 620.1865; found, 620.1868. Melting point: 157-158 °C.

*(E)-N-((5-(4-((3-chloro-4-((3-fluorobenzyl)oxy)phenyl)amino)quinazolin-6-yl)furan-2-yl)methyl)-N-(4-methoxybenzyl)-3-(pyridin-3-yl)acrylamide **25b**.*

^{1}H NMR (400 MHz, CDCl$_3$) δ 8.85 (d, J = 112.3 Hz, 1H), 8.61 (d, J = 9.9 Hz, 2H), 8.49 (s, 1H), 8.46 − 8.41 (m, 1H), 7.86 (s, 1H), 7.77 (d, J = 8.8 Hz, 1H), 7.71 (d, J = 11.8 Hz, 1H), 7.65 (d, J = 8.3 Hz, 1H), 7.58 (d, J = 10.1 Hz, 1H), 7.35 − 7.29 (m, 1H), 7.23 − 7.14 (m, 5H), 7.09 (d, J = 8.0 Hz, 1H), 6.98 (t, J = 8.4 Hz, 1H), 6.90 (d, J = 15.0 Hz, 1H), 6.85 (d, J = 8.4 Hz, 2H), 6.80 (d, J = 8.1 Hz, 1H), 6.64 (d, J = 12.0 Hz, 1H), 6.27 (d, J = 40.1 Hz, 1H), 5.06 (s, 2H), 4.70 − 4.64 (m, 3H), 4.54 − 4.45 (m, 1H), 3.72 (s, 3H). ^{13}C NMR (100 MHz,

CDCl$_3$) δ 166.70, 164.24, 161.79, 159.38, 154.82, 152.95, 150.96, 150.62, 149.28, 140.63, 139.12, 134.41, 132.65, 130.64, 130.22, 130.14, 129.76, 128.92, 128.77, 128.46, 127.88, 127.74, 125.07, 123.67, 123.37, 122.47, 122.44, 122.23, 119.14, 115.43, 115.01, 114.80, 114.50, 114.26, 114.10, 113.88, 111.90, 107.09, 70.40, 55.30, 50.22, 42.30. Yield: 39 mg, 64%. HRMS (ESI) m/z: calcd for C$_{42}$H$_{33}$ClFN$_5$O$_4$ [M + H] $^+$, 726.2283; found, 726.2297. Melting point: 155-157 °C.

(E)-N-((5-(4-((3-chloro-4-((3-fluorobenzyl)oxy)phenyl)amino)quinazolin-6-yl)furan-2-yl)methyl)-N-(2-(methylsulfonyl)ethyl)-3-(pyridin-3-yl)acrylamide **25c**.

^{1}H NMR (400 MHz, CDCl$_3$) δ 8.77 (d, *J* = 15.0 Hz, 1H), 8.68 (s, 1H), 8.59 (d, *J* = 4.1 Hz, 1H), 8.38 (d, *J* = 10.0 Hz, 2H), 7.93 (d, *J* = 8.8 Hz, 1H), 7.87 − 7.80 (m, 3H), 7.67 (dd, *J* = 24.1, 12.1 Hz, 2H), 7.37 − 7.31 (m, 2H), 7.22 (d, *J* = 10.0 Hz, 2H), 7.05 (d, *J* = 15.1 Hz, 1H), 6.99 (dd, *J* = 16.4, 8.6 Hz, 2H), 6.74 (s, 1H), 6.50 (d, *J* = 28.4 Hz, 1H), 5.15 (s, 2H), 4.78 (s, 2H), 4.24 (d, *J* = 56.8 Hz, 2H), 3.53 (s, 2H), 2.98 (s, 3H). ^{13}C NMR (100 MHz, CDCl$_3$) δ 166.44, 164.26, 161.81, 157.95, 155.06, 153.80, 150.90, 150.07, 149.17, 140.60, 139.14, 134.58, 132.58, 130.24, 130.16, 129.29, 128.90, 125.05, 123.84, 123.27, 122.50, 122.47, 122.23, 118.58, 115.58, 115.03, 114.82, 114.31, 114.13, 113.90, 111.16, 107.34, 70.45, 52.47, 46.50, 42.30, 41.43. Yield: 24 mg, 40%. HRMS (ESI) m/z: calcd for C$_{37}$H$_{31}$ClFN$_5$O$_5$S [M + H] $^+$, 734.1616; found, 734.1620. Melting point: 161-163 °C.

(E)-N-((5-(4-((3-chloro-4-((3-fluorobenzyl)oxy)phenyl)amino)quinazolin-6-yl)furan-2-yl)methyl)-N-isopropyl-3-(pyridin-3-yl)acrylamide **25d**.

^{1}H NMR (400 MHz, CDCl$_3$) δ 9.05 (d, *J* = 69.8 Hz, 1H), 8.65 (s, 2H), 8.49 (d, *J* = 33.2 Hz, 1H), 8.39 (d, *J* = 14.5 Hz, 1H), 7.91 (dd, *J* = 14.1, 9.1 Hz, 1H), 7.71 (dd, *J* = 42.2, 16.9 Hz, 4H), 7.55 − 7.48 (m, 1H), 7.34 − 7.30 (m, 1H), 7.18 (t, *J* = 7.4 Hz, 2H), 7.02 − 6.96 (m, 2H), 6.83 (t, *J* = 7.9 Hz, 1H), 6.57 (d, *J* = 36.2 Hz, 1H), 6.24 (d, *J* = 12.9 Hz, 1H), 5.03 (d, *J* = 7.9 Hz, 2H), 4.53 (d, *J* = 18.0 Hz, 2H), 4.46 − 4.28 (m, 1H), 1.22 (dd, *J* = 54.4, 5.8 Hz, 6H). ^{13}C NMR (100 MHz, CDCl$_3$) δ 166.38, 164.16, 161.72, 158.08, 154.79, 152.52, 151.67, 150.84, 150.24, 149.18, 148.85, 139.45, 139.14, 134.53, 132.74, 130.95, 130.11, 128.64, 125.02, 123.71, 123.15, 122.42, 122.23, 120.73, 119.78, 115.61, 114.94, 114.73, 114.02, 113.80, 110.29, 107.42, 70.26, 49.19, 45.99, 21.59, 20.26. Yield: 40 mg, 63.8%. HRMS (ESI) m/z: calcd for C$_{37}$H$_{31}$ClFN$_5$O$_3$ [M + H] $^+$, 648.2178; found, 648.2175. Melting point: 158-160 °C.

(E)-N-((5-(4-((3-chloro-4-((3-fluorobenzyl)oxy)phenyl)amino)quinazolin-6-yl)furan-2-yl)methyl)-N-cyclopropyl-3-(pyridin-3-yl)acrylamide **25e**.

^{1}H NMR (400 MHz, CDCl$_3$) δ 8.69 (s, 1H), 8.63 (s, 1H), 8.54 (s, 2H), 8.31 (s, 1H), 7.92 (d, *J* = 8.7 Hz, 1H), 7.80 (s, 2H), 7.72 (d, *J* = 7.8 Hz, 1H), 7.66 (d, *J* = 15.6 Hz, 1H), 7.53 (d, *J* = 8.7 Hz, 1H), 7.35 (s, 1H), 7.32 (d, *J* = 5.9 Hz, 1H), 7.19 (t, *J* = 8.3 Hz, 2H), 7.00 (t, *J* = 8.4 Hz, 1H), 6.86 (d, *J* = 8.7 Hz, 1H), 6.64 (s, 1H), 6.33 (s, 1H), 5.06 (s, 2H), 4.71 (s, 2H), 2.81 (s, 1H), 1.05 − 0.89 (m, 4H). ^{13}C NMR (100 MHz, CDCl$_3$) δ 168.01, 164.23, 157.93, 154.74, 152.42, 151.69, 150.96, 150.52, 149.25, 139.25, 139.17, 139.10, 134.50, 132.55,

130.86, 130.21, 130.13, 128.98, 128.77, 128.68, 125.06, 123.70, 123.34, 122.46, 122.43, 122.21, 120.53, 115.46, 115.23, 114.99, 114.78, 114.20, 114.08, 113.86, 110.76, 107.29, 70.36, 43.70, 29.83, 9.71. Yield: 43.3 mg, 69%. HRMS (ESI) m/z: calcd for $C_{37}H_{29}ClFN_5O_3$ [M + H]$^+$, 646.2021; found, 646.2054. Melting point: 163-164 °C.

(E)-N-((5-(4-((3-chloro-4-((3-fluorobenzyl)oxy)phenyl)amino)quinazolin-6-yl)furan-2-yl)methyl)-N-ethyl-3-(pyridin-3-yl)acrylamide **25f**.

^{1}H NMR (400 MHz, CDCl$_3$) δ 8.71 (s, 1H), 8.65 (s, 1H), 8.56 (s, 1H), 8.36 (s, 1H), 7.94 (d, *J* = 8.1 Hz, 1H), 7.84 (d, *J* = 9.7 Hz, 2H), 7.74 (d, *J* = 14.8 Hz, 2H), 7.53 (t, *J* = 27.9 Hz, 1H), 7.34 (s, 2H), 7.21 (t, *J* = 8.5 Hz, 2H), 7.01 (s, 1H), 6.90 (d, *J* = 10.2 Hz, 2H), 6.68 (s, 1H), 6.40 (s, 1H), 5.10 (s, 2H), 4.70 (d, *J* = 27.0 Hz, 2H), 3.55 (d, *J* = 6.8 Hz, 2H), 1.24 (dd, *J* = 13.6, 6.9 Hz, 3H). ^{13}C NMR (100 MHz, CDCl$_3$) δ 165.94, 164.25, 161.80, 157.97, 154.82, 152.84, 151.17, 151.00, 150.58, 149.22, 140.18, 139.12, 134.46, 130.78, 130.23, 130.14, 129.01, 128.81, 128.55, 125.10, 123.70, 123.40, 122.44, 122.23, 118.98, 115.30, 114.80, 114.28, 114.10, 113.88, 111.37, 107.18, 70.42, 50.72, 42.42, 14.60. Yield: 46.9 mg, 74.4%. HRMS (ESI) m/z: calcd for $C_{36}H_{29}ClFN_5O_3$ [M + H]$^+$, 634.2021; found, 634.1989. Melting point: 163-165 °C.

(E)-N-((5-(4-((3-chloro-4-((3-fluorobenzyl)oxy)phenyl)amino)quinazolin-6-yl)furan-2-yl)methyl)-N-propyl-3-(pyridin-3-yl)acrylamide **25g**.

^{1}H NMR (400 MHz, CDCl$_3$) δ 8.60 (d, *J* = 40.4 Hz, 3H), 8.29 (d, *J* = 56.5 Hz, 1H), 7.93 (d, *J* = 5.9 Hz, 1H), 7.81 (d, *J* = 10.1 Hz, 2H), 7.71 (d, *J* = 11.7 Hz, 2H), 7.55 (d, *J* = 8.7 Hz, 1H), 7.39 − 7.26 (m, 2H), 7.19 (t, *J* = 8.4 Hz, 3H), 7.00 (t, *J* = 8.3 Hz, 1H), 6.89 (d, *J* = 15.8 Hz, 2H), 6.67 (d, *J* = 15.0 Hz, 1H), 6.34 (d, *J* = 18.4 Hz, 1H), 5.07 (s, 2H), 4.67 (d, *J* = 28.2 Hz, 2H), 3.48 − 3.42 (m, 2H), 1.68 − 1.61 (m, 2H), 0.96 − 0.89 (m, 3H). ^{13}C NMR (100 MHz, CDCl$_3$) δ 166.15, 164.23, 161.79, 158.00, 154.80, 152.75, 151.17, 150.97, 150.54, 149.16, 140.02, 139.11, 134.42, 132.61, 130.22, 130.13, 128.79, 128.57, 125.10, 123.34, 122.46, 122.43, 122.24, 119.07, 115.41, 115.00, 114.79, 114.22, 114.09, 113.87, 111.26, 107.20, 70.38, 49.44, 42.82, 22.63, 11.30. Yield: 40 mg, 64%. HRMS (ESI) m/z: calcd for $C_{37}H_{31}ClFN_5O_3$ [M + H]$^+$, 648.2178; found, 648.2175. Melting point: 162-163 °C.

4.3 NAMPT Enzyme Inhibition Assay. A dilution ten-fold higher than the final concentration of the compounds was prepared with 10% DMSO and 5μl of the dilution was added to a 50μl reaction so that the final concentration of DMSO is 1% in all reactions. All of the enzymatic reactions were conducted in duplicates at 30°C for 90 minutes in a 50 μl mixture containing 50 mM Tris-HCl, pH 8.0, 12.5 mM MgCl$_2$, 20 μM nicotinamide, 0.4 mM Phosphoribosyl pyrophosphate, 2 mM ATP, 30 μg/mL of alcohol dehydrogenase, 10 μg/mL of NMNAT, 1.5% alcohol, 1 mM DTT, 0.02% BSA, 0.01% Tween 20, and the test compound. Fluorescence intensity was measured at an excitation of 360 nm and an emission of 460 nm using a Tecan Infinite M1000 microplate reader. NAMPT activity assays were performed in duplicates at each concentration. The fluorescent intensity data were analyzed using the computer software, Graphpad Prism. In the absence of the compound, the fluorescent intensity (Ft) in each data set was defined as

100% activity. In the absence of NAMPT, the fluorescent intensity (Fb) in each data set was defined as 0% activity. The percent activity in the presence of each compound was calculated according to the following equation: %activity = (F-Fb)/(Ft-Fb), where F= the fluorescent intensity in the presence of the compound.

Assay	Enzyme Used (ng) / Reaction	Substrate
NAMPT	200	Nicotinamide 20 μM/
		Phosphoribosyl pyrophosphate 400 μM

4.4 Molecular docking. The structure of **20c** for this docking was constructed using ChemDraw Professional 17.0 software, and then the structure was imported into Schrodinger software to establish a database. After hydrogenation, structural optimization, and energy minimization, it was saved as the ligand molecular database for molecular docking. EGFR (PDB ID: 6JRX) target protein crystal structure from PDB database (https://www.rcsb.org/). The protein structure is processed on the Maestro 11.9 platform, using Schrodinger's Protein Preparation Wizard to process the protein, remove crystal water, add missing hydrogen atoms, repair missing bond information, repair missing peptide segments, and finally minimize energy and optimize the geometric structure of the protein[46-47]. Molecular docking is accomplished by the Glide module in Schrödinger Maestro software. Protein processing utilizes the Protein Preparation Wizard module. Finally, molecular docking and screening were performed using the Standard Precision (SP) method.

4.5 Anti-proliferation Inhibition Assay. Cell lines, SK-BR-3, T47D, MDA-MB-453, MDA-MB-468, MDA-MB-435 and NCI-N87 were purchased from ATCC. Cell lines, NCI-H1975-EGFR-L858R/T790M/C797S, Ba/F3-EGFR-Del19/T790M/C797S were from KYINNO BIOTECHNOLOGY CO., LTD. All cell lines were cultured at 37°C and 5% CO_2 in complete medium RMPI 1640, DMEM, DMEM-F12, 5A or L15 with 10% FBS. Method A: The growth inhibition of cells by compounds was detected by the SRB method. The specific steps are as follows: cells in the logarithmic growth phase are inoculated into a 96-well culture plate at an appropriate density, 100 μL per well. After overnight culture, different concentrations of drugs are added for 72 h. Three replicate wells are set for each concentration, and corresponding Concentrations of vehicle controls and cell-free zero wells. After the action, the adherent cells were poured out of the culture medium, and 10% (w/v) trichloroacetic acid (100 μL/well) was added for fixation at 4°C for 1 h, and then washed with distilled water five times. Add 100 μL of SRB solution (Sigma, St. Louis, MO, USA) (4 mg/mL, dissolved in 1% glacial acetic acid), incubate at room temperature for 15 min, and wash with 1% glacial acetic acid for five times to remove unbound After drying at room temperature, 150 μL of 10 mM pyrolysis solution was added to each well, and SpectraMax 190 (Sunnyvale, CA, USA) microplate reader was used to measure the optical density (OD value) at 560 nm wavelength. The rate of inhibition of cell proliferation by the compound was calculated by the following formula:

$$\text{Cell viability (\%)} = \frac{OD(sample) - OD(blank)}{OD(control) - OD(blank)} \times 100\%$$

IC$_{50}$ values were estimated by the four-parameter method. Each group of experiments was independently repeated three times, and three replicate wells were set for each concentration. Results are presented as Mean ± SD.

Method B: All cell lines were cultured in a complete medium at 37°C, with 5% CO$_2$. Cells in the logarithmic growth phase were harvested and counted using a platelet counter. Cell viability was detected by the trypan blue exclusion method to ensure cell viability was above 90%. The cells were then seeded in 96-well culture plates with 90 µL per well, for a total of 3000 cells. Cells in 96-well plates were cultured at 37°C and 5% CO$_2$. Nine concentration gradients were set for the compounds to be tested, the highest concentration was 10 µM, 3.16-fold dilution, and then transfer 10 µL of serially diluted compounds to the corresponding experimental wells of a 96-well cell plate. Three replicates were set for each drug concentration. The cells in the medicated 96-well plate were cultured for 72 hours, and then CTG analysis was performed. Thaw CTG reagent and equilibrate the cell plate to room temperature for 30 minutes. An equal volume of CTG solution was added to each well. Cells were lysed by shaking on an orbital shaker for 5 minutes. The cell plate was left at room temperature for 20 minutes to stabilize the luminescent signal. Read the luminescence value and collect the data. Data were analyzed using GraphPad Prism 7.0 software, and a dose-response curve was fitted to the data using nonlinear S-curve regression, from which IC$_{50}$ values were calculated.

Cell viability (%) = (Lum drug to be tested-Lum culture medium control)/ (Lum cell control-Lum culture medium control) ×100%.

4.6 Drug Endocytosis Assay. The MDA-MB-453 and SK-BR-3 cells in the logarithmic growth phase were inoculated into 12-well plates at the corresponding concentrations, with 1 mL of culture medium per well. After overnight incubation, 50µM of compounds were added to each well respectively. Cells and supernatants were collected after 5 min, 30 min, 1 h, 2 h, and 4 h. The supernatant was directly collected and centrifuged to remove the cells in the culture medium. After the cells were digested with trypsin, the culture medium was neutralized, and centrifuged at 1000 rpm for 5 min to remove the supernatant, washed with pre-cooled PBS and centrifuged to remove the supernatant, which was the cell pellet. Add 100 µL of cell lysate to the cell pellet, perform high-speed centrifugation (12000 r/min) at 4 °C, collect the supernatant, add 100 µL of methanol for protein precipitation, and perform high-speed centrifugation at 4 °C again (12000 r/min), the supernatant was filtered and analyzed by HPLC. Add 1 mL of methanol to the directly collected supernatant for protein precipitation, centrifuge at high speed (12000 r/min) at 4 °C, and filter the supernatant for HPLC analysis.

$$\text{Cellular internalization (\%)} = \frac{Cf \times Vf}{Ci \times Vi} \times 100\%$$

C_f is the final test concentration; V_f is the final volume; C_i is the initial test concentration; V_i is the initial volume.

References

1. Jaracz, S.; Chen, J.; Kuznetsova, L. V.; Ojima, I., Recent advances in tumor-targeting anticancer drug conjugates. *Bioorg Med Chem* **2005,** *13* (17), 5043-54.

2. Abdollahpour-Alitappeh, M.; Lotfinia, M.; Gharibi, T.; Mardaneh, J.; Farhadihosseinabadi, B.; Larki, P.; Faghfourian, B.; Sepehr, K. S.; Abbaszadeh-Goudarzi, K.; Abbaszadeh-Goudarzi, G.; Johari, B.; Zali, M. R.; Bagheri, N., Antibody-drug conjugates (ADCs) for cancer therapy: Strategies, challenges, and successes. *J Cell Physiol* **2019,** *234* (5), 5628-5642.

3. Baker, J. H.; Lindquist, K. E.; Huxham, L. A.; Kyle, A. H.; Sy, J. T.; Minchinton, A. I., Direct visualization of heterogeneous extravascular distribution of trastuzumab in human epidermal growth factor receptor type 2 overexpressing xenografts. *Clin Cancer Res* **2008,** *14* (7), 2171-9.

4. Girish, S.; Gupta, M.; Wang, B.; Lu, D.; Krop, I. E.; Vogel, C. L.; Burris Iii, H. A.; LoRusso, P. M.; Yi, J. H.; Saad, O.; Tong, B.; Chu, Y. W.; Holden, S.; Joshi, A., Clinical pharmacology of trastuzumab emtansine (T-DM1): an antibody-drug conjugate in development for the treatment of HER2-positive cancer. *Cancer Chemother Pharmacol* **2012,** *69* (5), 1229-40.

5. Perino, S.; Moreau, B.; Freda, J.; Cirello, A.; White, B. H.; Quinn, J. M.; Kriksciukaite, K.; Someshwar, A.; Romagnoli, J.; Robinson, M.; Movassaghian, S.; Cipriani, T.; Wooster, R.; Bilodeau, M. T.; Whalen, K. A., Novel Miniaturized Drug Conjugate Leverages HSP90-driven Tumor Accumulation to Overcome PI3K Inhibitor Delivery Challenges to Solid Tumors. *Mol Cancer Ther* **2020,** *19* (8), 1613-1622.

6. Cai, X.; Zhai, H. X.; Wang, J.; Forrester, J.; Qu, H.; Yin, L.; Lai, C. J.; Bao, R.; Qian, C., Discovery of 7-(4-(3-ethynylphenylamino)-7-methoxyquinazolin-6-yloxy)-N-hydroxyheptanamide (CUDc-101) as a potent multi-acting HDAC, EGFR, and HER2 inhibitor for the treatment of cancer. *J Med Chem* **2010,** *53* (5), 2000-9.

7. Prenzel, N.; Fischer, O. M.; Streit, S.; Hart, S.; Ullrich, A., The epidermal growth factor receptor family as a central element for cellular signal transduction and diversification. *Endocrine-related cancer Endocr Relat Cancer Endocr. Relat. Cancer* **2001,** *8* (1), 11-31.

8. Lurje, G.; Lenz, H. J., EGFR signaling and drug discovery. *Oncology* **2009,** *77* (6), 400-10.

9. Schjoldager, K. T.; Narimatsu, Y.; Joshi, H. J.; Clausen, H., Global view of human protein glycosylation pathways and functions. *Nat Rev Mol Cell Biol* **2020,** *21* (12), 729-749.

10. Yang, F.; Ai, W.; Jiang, F.; Liu, X.; Huang, Z.; Ai, S., Preclinical Evaluation of an Epidermal Growth Factor Receptor-Targeted Doxorubicin-Peptide Conjugate: Toxicity, Biodistribution, and Efficacy in Mice. *J Pharm Sci* **2016,** *105* (2), 639-649.

11. Chou, C. W.; Wu, M. S.; Huang, W. C.; Chen, C. C., HDAC inhibition decreases the expression of EGFR in colorectal cancer cells. *PLoS One* **2011,** *6* (3), e18087.

12. Gerber, D. E., EGFR Inhibition in the Treatment of Non-Small Cell Lung Cancer. *Drug Dev Res* **2008,** *69* (6), 359-372.

13. Guardiola, S.; Varese, M.; Sanchez-Navarro, M.; Giralt, E., A Third Shot at EGFR: New Opportunities in Cancer Therapy. *Trends Pharmacol Sci* **2019,** *40* (12), 941-955.

14. Martinelli, E.; Ciardiello, D.; Martini, G.; Troiani, T.; Cardone, C.; Vitiello, P. P.; Normanno, N.; Rachiglio, A. M.; Maiello, E.; Latiano, T.; De Vita, F.; Ciardiello, F., Implementing anti-epidermal growth factor receptor (EGFR) therapy in metastatic colorectal cancer: challenges and future perspectives. *Ann Oncol* **2020,** *31* (1), 30-40.

15. Mendelsohn, J.; Baselga, J., Status of epidermal growth factor receptor antagonists in the biology and treatment of cancer. *Journal of Clinical Oncology* **2003,** *21* (14), 2787-2799.

16. Hynes, N. E.; Lane, H. A., ERBB receptors and cancer: the complexity of targeted inhibitors. *Nat Rev Cancer* **2005,** *5* (5), 341-54.

17. Xia, G.; Chen, W.; Zhang, J.; Shao, J.; Zhang, Y.; Huang, W.; Zhang, L.; Qi, W.; Sun, X.; Li, B.; Xiang, Z.; Ma, C.; Xu, J.; Deng, H.; Li, Y.; Li, P.; Miao, H.; Han, J.; Liu, Y.; Shen, J.; Yu, Y., A chemical tuned strategy to develop novel irreversible EGFR-TK inhibitors with improved safety and pharmacokinetic profiles. *J Med Chem* **2014,** *57* (23), 9889-900.

18. Li, Z. R.; Suo, F. Z.; Hu, B.; Guo, Y. J.; Fu, D. J.; Yu, B.; Zheng, Y. C.; Liu, H. M., Identification of osimertinib (AZD9291) as a lysine specific demethylase 1 inhibitor. *Bioorg Chem* **2019,** *84*, 164-169.

19. Tan, L.; Zhang, J.; Wang, Y.; Wang, X.; Wang, Y.; Zhang, Z.; Shuai, W.; Wang, G.; Chen, J.; Wang, C.; Ouyang, L.; Li, W., Development of Dual Inhibitors Targeting Epidermal Growth Factor Receptor in Cancer Therapy. *J Med Chem* **2022**.

20. Sepay, N.; Mondal, R.; Al-Muhanna, M. K.; Saha, D., Identification of natural flavonoids as novel EGFR inhibitors using DFT, molecular docking, and molecular dynamics. *New Journal of Chemistry* **2022**.

21. Palacios, D. S.; Meredith, E. L.; Kawanami, T.; Adams, C. M.; Chen, X.; Darsigny, V.; Palermo, M.; Baird, D.; George, E. L.; Guy, C.; Hewett, J.; Tierney, L.; Thigale, S.; Wang, L.; Weihofen, W. A., Scaffold Morphing Identifies 3-Pyridyl Azetidine Ureas as Inhibitors of Nicotinamide Phosphoribosyltransferase (NAMPT). *ACS Med Chem Lett* **2019,** *10* (11), 1524-1529.

22. Imai, S., "Clocks" in the NAD World: NAD as a metabolic oscillator for the regulation of metabolism and aging. *Biochim Biophys Acta* **2010,** *1804* (8), 1584-90.

23. Dahl, T. B.; Holm, S.; Aukrust, P.; Halvorsen, B., Visfatin/NAMPT: a multifaceted molecule with diverse roles in physiology and pathophysiology. *Annu Rev Nutr* **2012,** *32*, 229-43.

24. Garten, A.; Petzold, S.; Korner, A.; Imai, S.; Kiess, W., Nampt: linking NAD biology, metabolism and cancer. *Trends Endocrinol Metab* **2009,** *20* (3), 130-8.

25. Xiao, Y.; Kwong, M.; Daemen, A.; Belvin, M.; Liang, X.; Hatzivassiliou, G.; O'Brien, T., Metabolic Response to NAD Depletion across Cell Lines Is Highly Variable. *PLoS One* **2016,** *11* (10), e0164166.

26. Wang, W.; Elkins, K.; Oh, A.; Ho, Y. C.; Wu, J.; Li, H.; Xiao, Y.; Kwong, M.; Coons, M.; Brillantes, B.; Cheng, E.; Crocker, L.; Dragovich, P. S.; Sampath, D.; Zheng, X.; Bair, K. W.; O'Brien, T.; Belmont, L. D., Structural basis for resistance to diverse classes of NAMPT inhibitors. *PLoS One* **2014,** *9* (10), e109366.

27. Gehrke, I.; Bouchard, E. D. J.; Beiggi, S.; Poeppl, A. G.; Johnston, J. B.; Gibson, S. B.; Banerji, V., On-Target Effect of FK866, a Nicotinamide Phosphoribosyl Transferase Inhibitor, by Apoptosis-Mediated Death in Chronic Lymphocytic Leukemia Cells. *Clinical Cancer Research* **2014,** *20* (18), 4861-4872.

28. Karpov, A. S.; Abrams, T.; Clark, S.; Raikar, A.; D'Alessio, J. A.; Dillon, M. P.; Gesner, T. G.; Jones, D.; Lacaud, M.; Mallet, W.; Martyniuk, P.; Meredith, E.; Mohseni, M.; Nieto-Oberhuber, C. M.; Palacios, D.; Perruccio, F.; Piizzi, G.; Zurini, M.; Bialucha, C. U., Nicotinamide Phosphoribosyltransferase Inhibitor as a Novel Payload for Antibody-Drug Conjugates. *ACS Med Chem Lett* **2018,** *9* (8), 838-842.

29. von Heideman, A.; Berglund, A.; Larsson, R.; Nygren, P., Safety and efficacy of NAD depleting cancer drugs: results of a phase I clinical trial of CHS 828 and overview of published data. *Cancer Chemother Pharmacol* **2010,** *65* (6), 1165-72.

30. Woodburn, J. R., The Epidermal Growth Factor Receptor and Its Inhibition in Cancer Therapy. *Pharmacology & Therapeutics* **1999,** *82* (2), 241-250.

31. Stamos, J.; Sliwkowski, M. X.; Eigenbrot, C., Structure of the epidermal growth factor receptor kinase domain alone and in complex with a 4-anilinoquinazoline inhibitor. *J Biol Chem* **2002,** *277* (48), 46265-72.

32. Cheng, M.; Yu, X.; Lu, K.; Xie, L.; Wang, L.; Meng, F.; Han, X.; Chen, X.; Liu, J.; Xiong, Y.; Jin, J., Discovery of Potent and Selective Epidermal Growth Factor Receptor (EGFR) Bifunctional Small-Molecule Degraders. *J Med Chem* **2020,** *63* (3), 1216-1232.

33. Khan, J. A.; Tao, X.; Tong, L., Molecular basis for the inhibition of human NMPRTase, a novel target for anticancer agents. *Nat Struct Mol Biol* **2006,** *13* (7), 582-8.

34. Sampath, D.; Zabka, T. S.; Misner, D. L.; O'Brien, T.; Dragovich, P. S., Inhibition of nicotinamide phosphoribosyltransferase (NAMPT) as a therapeutic strategy in cancer. *Pharmacol Ther* **2015,** *151*, 16-31.

35. Subik, K.; Lee, J. F.; Baxter, L.; Strzepek, T.; Costello, D.; Crowley, P.; Xing, L.; Hung, M. C.; Bonfiglio, T.; Hicks, D. G.; Tang, P., The Expression Patterns of ER, PR, HER2, CK5/6, EGFR, Ki-67 and AR by Immunohistochemical Analysis in Breast Cancer Cell Lines. *Breast cancer : basic and clinical research* **2010,** *4*, 35-41.

36. Zajdel, A.; Nycz, J.; Wilczok, A., Lapatinib enhances paclitaxel toxicity in MCF-7, T47D, and MDA-MB-321 breast cancer cells. *Toxicol In Vitro* **2021,** *75*, 105200.

37. Yang, X.; Huang, C.; Chen, R.; Zhao, J., Resolving Resistance to Osimertinib Therapy With Afatinib in an NSCLC Patient With EGFR L718Q Mutation. *Clin Lung Cancer* **2020,** *21* (4), e258-e260.

38. Ho, C. C.; Liao, W. Y.; Lin, C. A.; Shih, J. Y.; Yu, C. J.; Yang, J. C., Acquired BRAF V600E Mutation as Resistant Mechanism after Treatment with Osimertinib. *Journal of thoracic oncology : official publication of the International Association for the Study of Lung Cancer* **2017,** *12* (3), 567-572.

39. Wang, S.; Cang, S.; Liu, D., Third-generation inhibitors targeting EGFR T790M mutation in advanced non-small cell lung cancer. *J Hematol Oncol* **2016,** *9*, 34.

40. Wang, S.; Song, Y.; Yan, F.; Liu, D., Mechanisms of resistance to third-generation EGFR tyrosine kinase inhibitors. *Front Med* **2016,** *10* (4), 383-388.

41. Tang, X.; Cheng, L.; Li, G.; Yan, Y. M.; Su, F.; Huang, D. L.; Zhang, S.; Liu, Z.; Qian, M.; Li, J.; Cheng, Y. X.; Liu, B., A small-molecule compound D6 overcomes EGFR-T790M-mediated resistance in non-small cell lung cancer. *Commun Biol* **2021,** *4* (1), 1391.

42. Zhang, H.; Xie, R.; Ai-furas, H.; Li, Y.; Wu, Q.; Li, J.; Xu, F.; Xu, T., Design, Synthesis, and Biological Evaluation of Novel EGFR PROTACs Targeting Del19/T790M/C797S Mutation. *ACS Medicinal Chemistry Letters* **2022,** *13* (2), 278-283.

43. Du, Y.; Chen, Y.; Wang, Y.; Chen, J.; Lu, X.; Zhang, L.; Li, Y.; Wang, Z.; Ye, G.; Zhang, G., HJM-561, a potent, selective and orally bioavailable EGFR PROTAC that overcomes osimertinib-resistant EGFR triple mutations. *Molecular Cancer Therapeutics* **2022**.

44. Yonesaka, K.; Kobayashi, Y.; Hayashi, H.; Chiba, Y.; Mitsudomi, T.; Nakagawa, K., Dual blockade of EGFR tyrosine kinase using osimertinib and afatinib eradicates EGFRmutant Ba/F3 cells. *Oncology reports* **2019,** *41* (2), 1059-1066.

45. Kwon, Y. S.; Nam, K. S.; Kim, S., Tamoxifen overcomes the trastuzumab-resistance of SK-BR-3 tumorspheres by targeting crosstalk between cytoplasmic estrogen receptor alpha and the EGFR/HER2 signaling pathway. *Biochem Pharmacol* **2021,** *190*, 114635.

46. Rajeswari, M.; Santhi, N.; Bhuvaneswari, V., Pharmacophore and Virtual Screening of JAK3 inhibitors. *Bioinformation* **2014,** *10* (3), 157-63.

47. Fazi, R.; Tintori, C.; Brai, A.; Botta, L.; Selvaraj, M.; Garbelli, A.; Maga, G.; Botta, M., Homology Model-Based Virtual Screening for the Identification of Human Helicase DDX3 Inhibitors. *Journal of chemical information and modeling* **2015,** *55* (11), 2443-54.
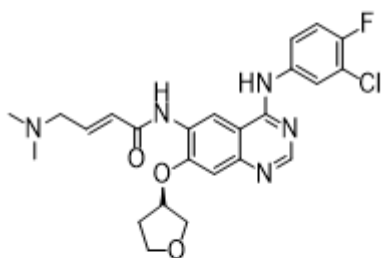
Schemes

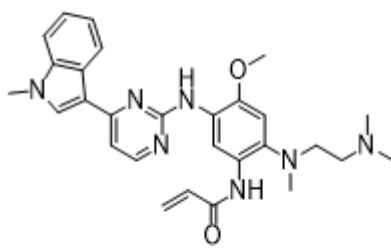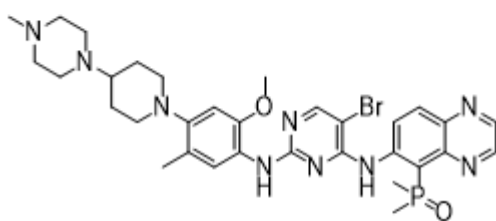Schemes 1-4 are available in the Supplementary Files section.
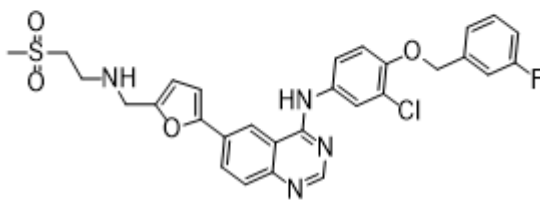
Figures
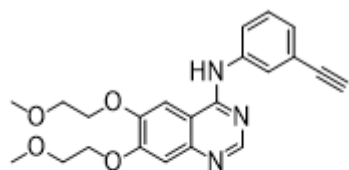
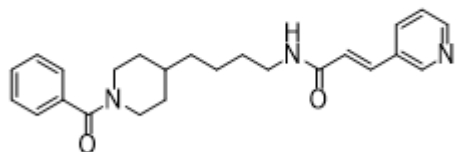Erlotinib
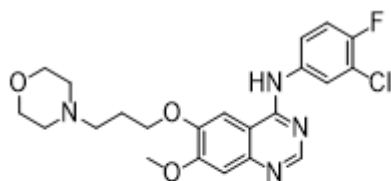
Gefitinib

Afatinib
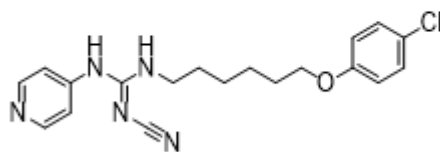
Osimertinib(AZD9291)

TQB3805

Lapatinib

FK866

CHS828

Figure 1

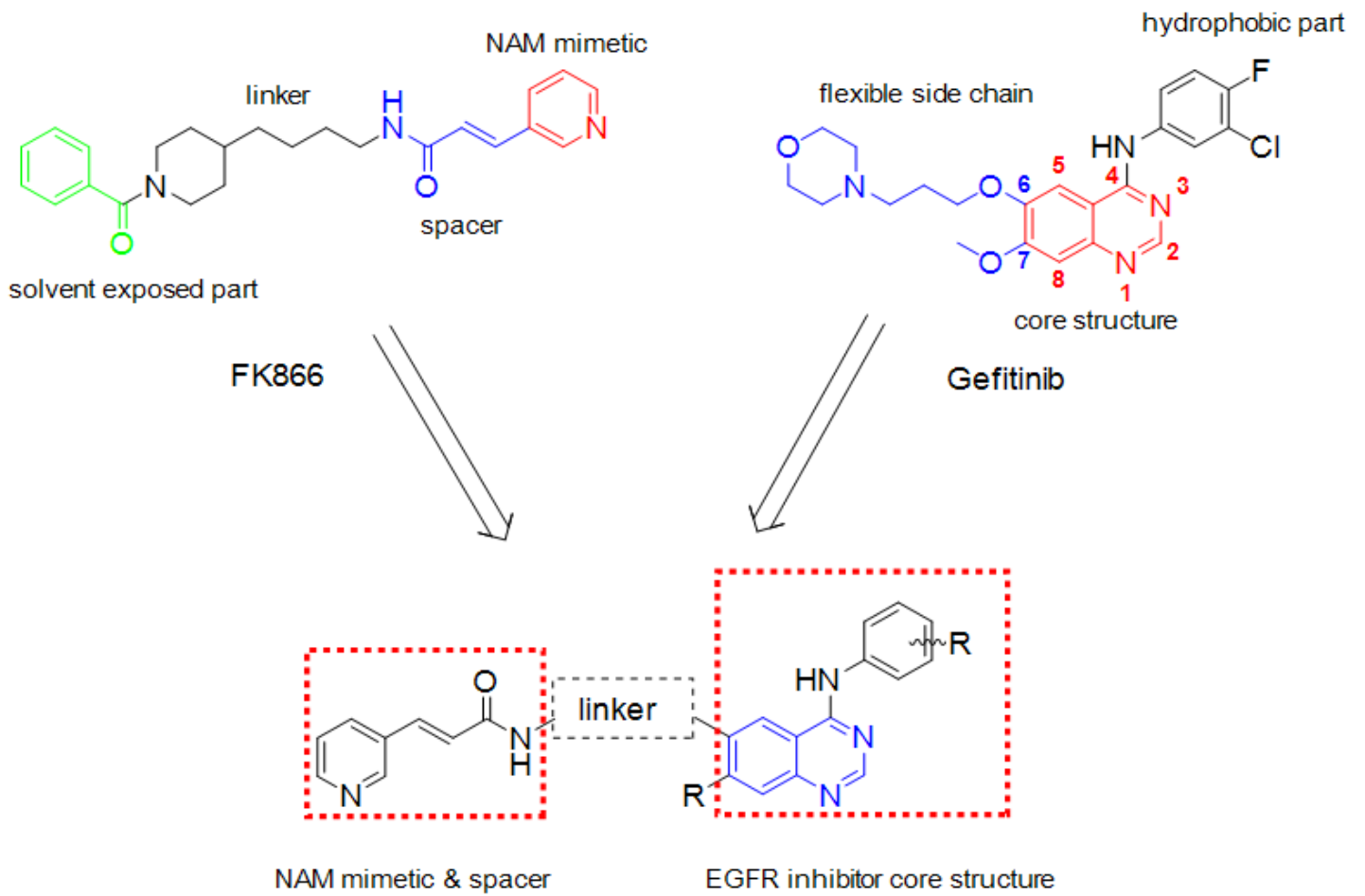Structures of reported EGFR&HER2 inhibitors and NAMPT inhibitors

Figure 2

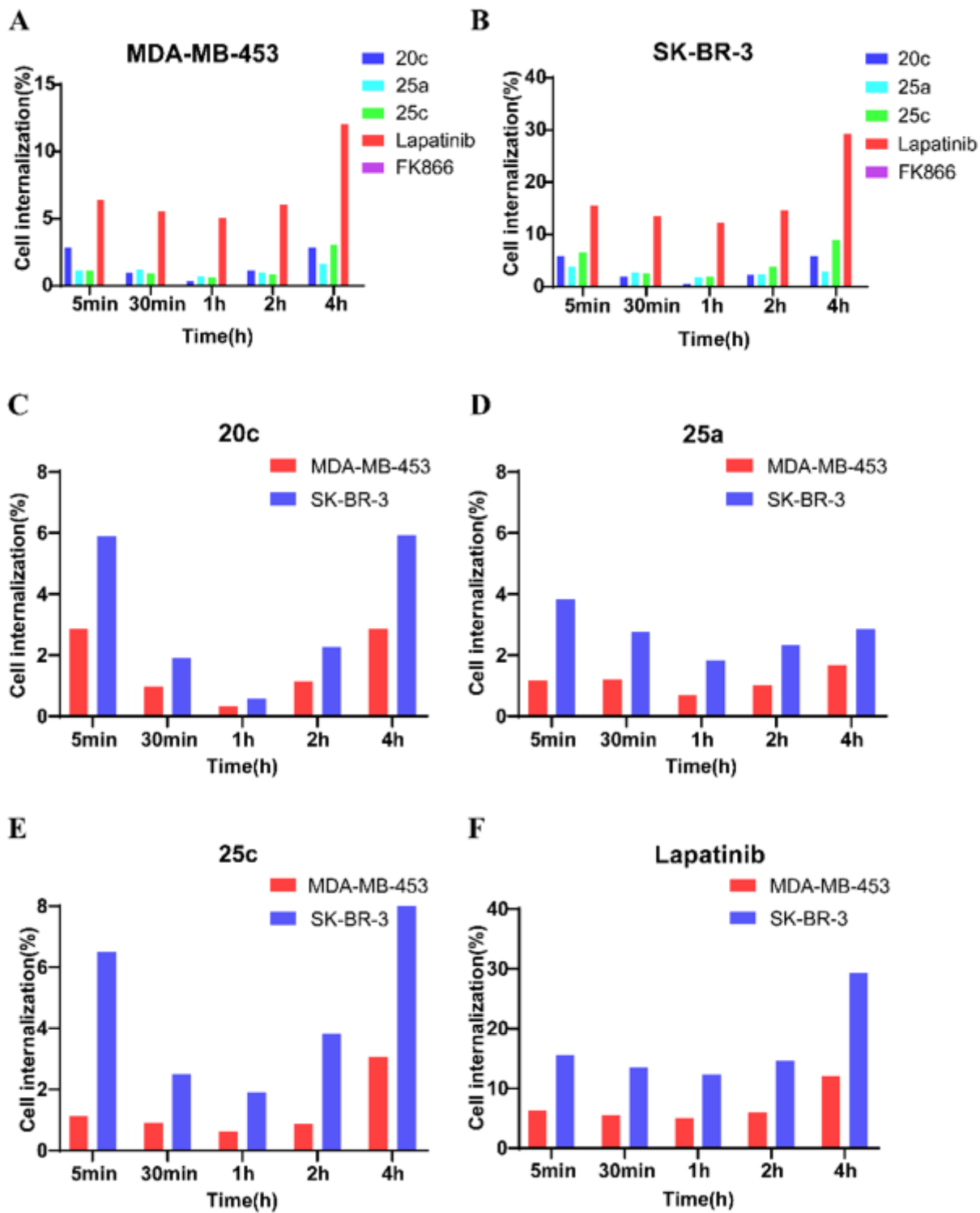Illustration of designed EGFR&HER2-NAMPT drug conjugates

Figure 4

Amount of cellular internalization. All compounds are selective to cells with high expression of EGFR and HER2, preferring to enter SK-BR-3 cells rather than MDA-MB-453 cells.

Supplementary Files

This is a list of supplementary files associated with this preprint. Click to download.

- Scheme1.png
- Scheme2.png
- Scheme3.png
- Scheme4.png
- Supportinginformation.docx